Title

Observations of total $RONO_2$ over the boreal forest: NO_x sinks and HNO_3 sources

Journal

Atmospheric Chemistry and Physics, 13(9)

ISSN

1680-7324

Authors

Browne, E. C
Min, K.-E.
Wooldridge, P. J
et al.

Publication Date

2013-05-02

DOI

10.5194/acp-13-4543-2013

Atmos. Chem. Phys., 13, 4543–4562, 2013
www.atmos-chem-phys.net/13/4543/2013/
doi:10.5194/acp-13-4543-2013

Atmospheric Chemistry and Physics Open Access

Observations of total $RONO_2$ over the boreal forest: NO_x sinks and HNO_3 sources

E. C. Browne[1], K.-E. Min[2,*], P. J. Wooldridge[1], E. Apel[3], D. R. Blake[4], W. H. Brune[5], C. A. Cantrell[3], M. J. Cubison[6,], G. S. Diskin[7], J. L. Jimenez[6], A. J. Weinheimer[3], P. O. Wennberg[8], A. Wisthaler[9], and R. C. Cohen[1,2]**

[1]Department of Chemistry, University of California Berkeley, Berkeley, CA, USA
[2]Department of Earth and Planetary Science, University of California Berkeley, Berkeley, CA, USA
[3]Atmospheric Chemistry Division, National Center for Atmospheric Research, Boulder, CO, USA
[4]Department of Chemistry, University of California Irvine, Irvine, CA, USA
[5]Department of Meteorology, Pennsylvania State University, University Park, PA, USA
[6]Cooperative Institute for Research in the Environmental Sciences (CIRES) and Department of Chemistry and Biochemistry, University of Colorado, Boulder, CO, USA
[7]NASA Langley Research Center, Hampton, Virginia, USA
[8]Division of Geology and Planetary Sciences, California Institute of Technology, Pasadena, CA, USA
[9]Institut für Ionenphysik & Angewandte Physik, University of Innsbruck, Innsbruck, Austria
[*]now at: NOAA Earth System Research Laboratory and Cooperative Institute for Research in Environmental Sciences, University of Colorado, Boulder, USA
[**]now at: Tofwerk AG, Thun, Switzerland

Correspondence to: R. C. Cohen (rccohen@berkeley.edu)
and E. C. Browne (ecbrowne@mit.edu)

Received: 11 December 2012 – Published in Atmos. Chem. Phys. Discuss.: 4 January 2013
Revised: 8 April 2013 – Accepted: 12 April 2013 – Published: 2 May 2013

Abstract. In contrast with the textbook view of remote chemistry where HNO_3 formation is the primary sink of nitrogen oxides, recent theoretical analyses show that formation of $RONO_2$ (ΣANs) from isoprene and other terpene precursors is the primary net chemical loss of nitrogen oxides over the remote continents where the concentration of nitrogen oxides is low. This then increases the prominence of questions concerning the chemical lifetime and ultimate fate of ΣANs. We present observations of nitrogen oxides and organic molecules collected over the Canadian boreal forest during the summer which show that ΣANs account for $\sim$ 20 % of total oxidized nitrogen and that their instantaneous production rate is larger than that of HNO_3. This confirms the primary role of reactions producing ΣANs as a control over the lifetime of NO_x ($NO_x = NO + NO_2$) in remote, continental environments. However, HNO_3 is generally present in larger concentrations than ΣANs indicating that the atmospheric lifetime of ΣANs is shorter than the HNO_3 lifetime. We investigate a range of proposed loss mechanisms that would explain the inferred lifetime of ΣANs finding that in combination with deposition, two processes are consistent with the observations: (1) rapid ozonolysis of isoprene nitrates where at least $\sim$ 40 % of the ozonolysis products release NO_x from the carbon backbone and/or (2) hydrolysis of particulate organic nitrates with HNO_3 as a product. Implications of these ideas for our understanding of NO_x and NO_y budget in remote and rural locations are discussed.

1 Introduction

In remote, continental regions, isoprene, terpenes and other biogenic volatile organic compounds (BVOCs) rival CH_4 and CO as controls over the free radical chemistry of the atmospheric boundary layer, affecting global distributions of oxidants (OH, O_3, NO_3) and oxidant precursors (e.g. NO_x,

HCHO) (e.g. Fuentes et al., 2000). In turn, these oxidants control the burden of tropospheric ozone and of both short (e.g. isoprene) and long-lived (e.g. CH_4, CH_3Br) organic compounds thus impacting climate. Consequently, the oxidative chemistry of BVOC has been the subject of extensive research. Recent advances in laboratory and field measurements have focused on the products of BVOC oxidation and have inspired renewed examination of how the mechanisms of BVOC oxidation affect atmospheric composition. In particular, the impact of BVOC on the HO_x budget has been highlighted (e.g. Thornton et al., 2002; Lelieveld et al., 2008; Hofzumahaus et al., 2009; Stavrakou et al., 2010; Stone et al., 2011; Whalley et al., 2011; Mao et al., 2012; Paulot et al., 2012; Taraborrelli et al., 2012).

Oxidation of BVOC by OH results in peroxy radicals, which may react with NO_x ($NO_x = NO + NO_2$), with other peroxy radicals (RO_2 or HO_2), or – in some cases – may isomerize (potentially regenerating OH). The reaction of peroxy radicals with NO_2 results in the formation of peroxy nitrates (RO_2NO_2) – a class of molecules which generally act as temporary reservoirs of NO_x and serve to transport NO_x on regional and global scales. Reaction of peroxy radicals with NO generally acts to propagate the ozone production cycle (R1a); however, a minor channel of the Reaction (R1b) which proceeds with the efficiency α (also known as the branching ratio), results in the formation of organic nitrates ($RONO_2$).

$$RO_2 + NO \rightarrow RO + NO_2 \quad (1-\alpha) \qquad \text{(R1a)}$$

$$RO_2 + NO \rightarrow RONO_2 \quad (\alpha) \qquad \text{(R1b)}$$

Calculations with box and chemical transport models (CTMs) have shown that organic nitrates play a significant role in the NO_x and O_3 budgets (e.g. Trainer et al., 1991; Chen et al., 1998; Horowitz et al., 1998, 2007; Liang et al., 1998; von Kuhlmann et al., 2004; Fiore et al., 2005; Wu et al., 2007; Paulot et al., 2012). In Browne and Cohen (2012) we have shown that at NO_x concentrations typical of remote and rural environments; the formation of ΣANs is the dominant instantaneous NO_x sink even at modest concentrations of BVOC. However, the net impact on O_3 and NO_x depends on the extent to which ΣANs act as a permanent versus temporary NO_x sink, as has been shown in numerous models (e.g. von Kuhlmann et al., 2004; Fiore et al., 2005, 2011; Horowitz et al., 2007; Ito et al., 2009; Paulot et al., 2012). The lifetime and fate of ΣANs remains one of the outstanding questions about their chemistry; compared to other aspects of the NO_y, HO_x and VOC chemistry, there has been limited research on products of ΣANs oxidation. Even for those nitrates whose oxidation products and yields have been measured, these measurements have occurred under conditions where the resulting peroxy radicals react primarily with NO and not with HO_2 or RO_2 (which are the expected reactions in the low NO_x conditions of the boreal forest). As recently pointed out by Elrod and co-workers (Darer et al., 2011; Hu et al., 2011), ΣANs may also be removed via hydrolysis in aerosol with an assumed product of NO_3^-. This uncertainty in the fate of ΣANs results in large uncertainties in global ozone budgets. For instance, recent modeling studies have found that the ozone response to increasing isoprene emissions (as predicted in a warmer climate) is highly sensitive to the fate of isoprene nitrates (Ito et al., 2009; Weaver et al., 2009).

Here, we use observations, collected aboard the NASA DC-8 aircraft, of a suite of nitrogen oxides, organic molecules, and oxidants (OH and O_3) from the July 2008 NASA ARCTAS (Arctic Research of the Composition of the Troposphere from Aircraft and Satellites) campaign over the Canadian boreal forest, to examine the extent to which the organic nitrate products of BVOC oxidation control the lifetime of NO_x in the remote continental boundary layer. We find that the production of ΣANs is dominated by biogenic molecules and is generally larger than the production of HNO_3. Using the concentration measurements in conjunction with the production rates, our measurements also provide a constraint on the ratio of the ΣANs lifetime to the HNO_3 lifetime over the boreal forest. We examine the loss processes of ΣANs find that both deposition and chemical loss processes (including oxidation of isoprene nitrates and hydrolysis of ΣANs in aerosol) are important. We find that the ozonolysis of isoprene nitrates is the largest gas-phase sink and we find that the particle phase hydrolysis of ΣANs, which produces HNO_3, may be both an important loss process for ΣANs and a significant source of HNO_3. The branching of ΣANs loss between the processes that return NO_x to the pool of available free radicals (e.g. oxidation) and those that remove NO_x from the atmosphere (e.g. deposition, hydrolysis) has important consequences for regional and global NO_x, O_3, and OH.

2 ARCTAS measurements

The NASA ARCTAS experiment was designed to study processes influencing Arctic chemistry and climate and has been described in detail previously by Jacob et al. (2010). In this analysis we use measurements from the summer portion of the campaign over the Canadian boreal forest (June–July 2008). These measurements were made aboard the NASA DC-8 aircraft which contained instrumentation for an extensive suite of gas and aerosol measurements.

NO_2, total peroxy nitrates (ΣPNs), and total organic nitrates (ΣANs) were measured aboard the DC-8 using thermal dissociation-laser induced fluorescence (TD-LIF). The instrument has been described in detail elsewhere (Day et al., 2002; Wooldridge et al., 2010) and the specific configuration used during ARCTAS has been described in Browne et al. (2011). Briefly, a two-cell TD-LIF with supersonic expansion (Thornton et al., 2000; Cleary et al., 2002; Day et al., 2002; Wooldridge et al., 2010) was deployed for ARCTAS. We use a 7 kHz, Q-switched, frequency doubled Nd:YAG

laser to pump a tunable dye laser (pyrromethene 597 in isopropanol) tuned to a 585 nm absorption in the NO_2 spectrum. We reject prompt scatter using time gated detection and eliminate scattered light at < 700 nm using bandpass filters. Fluorescence is imaged onto a red sensitive photomultiplier tube and counts are recorded at 4 Hz. The dye laser is tuned on and off an isolated rovibronic feature in the NO_2 spectrum, spending 9 s on the peak of the NO_2 absorbance and 3 s in an off-line position in the continuum of the NO_2 absorption. The difference between the two signals is directly proportional to the NO_2 concentration. We calibrate at least every two hours during a level flight leg using a 4.5 ppm NO_2 reference standard diluted to $\sim$ 2–8 ppbv in zero air.

The sample flow was split in thirds with one third directed to detection cell 1, where ambient NO_2 was continuously measured. The remaining flow was equally split between the measurement of total peroxy nitrates (ΣPNs) and total organic nitrates (ΣANs) which are detected by thermal conversion to NO_2 in heated quartz tubes. ΣPNs were converted to NO_2 at $\sim 200\,^{\circ}$C and ΣANs at $\sim 375\,^{\circ}$C, which is sufficient to dissociate ΣANs as well as any semivolatile aerosol phase organic nitrates (Rollins et al., 2010b). We do not detect non-volatile nitrates (i.e. $NaNO_3$). The resulting NO_2 of both heated channels ($NO_2+\Sigma$PNs or $NO_2+\Sigma$PNs$+\Sigma$ANs) was measured in cell 2. The duty cycle of cell 2 was evenly split between the measurement of ΣPNs and of ΣANs and alternated between the two either every 12 s or every 24 s. The 9 s average from each on-line block was reported to the data archive which is publically available at http://www-air.larc.nasa.gov/missions/arctas/arctas.html.

ΣPNs are calculated from the difference in signal between the ambient temperature and 200 °C channel and likewise, ΣANs are calculated from the difference in signal between the 375 °C ($NO_2 + \Sigma$PNs $+ \Sigma$ANs) and the 200 °C ($NO_2+\Sigma$PNs). The detection limit (defined as signal to noise of 2 for the 9 s average) of the ΣANs signal is directly related to the magnitude of the $NO_2 + \Sigma$PNs (NP) signal and during ARCTAS was on average < 20 pptv for a 200 pptv NP signal. The ΣANs signal also requires interpolation of the NP signal which we calculate using a weighted sum of a linear interpolation of the NP signal (weight $\sim 1/3$) and an interpolation of the ratio of NP to NO_2 signal scaled to the measured NO_2. The uncertainty in the ΣANs measurement depends both on the magnitude and the variability of the NP signal. On average, the NP signal varied by less than 20 % on the timescale of the ΣANs measurements. An example time series of the ΣANs and ΣPNs data is shown in Fig. 1.

In the analysis below we use measurements only between 10 and 18 local solar time which enables us to neglect the possible interference from $ClNO_2$ (Thaler et al., 2011) since $ClNO_2$ is rapidly photolyzed during daylight hours.

In addition to the core measurement of ΣANs, described above, we use the measurements listed in Table 1 in our analysis. We use the merged data set from flights over the boreal forest of Canada that took place 29 June–13 July 2008 averaged to the 60 s time base (version 13).

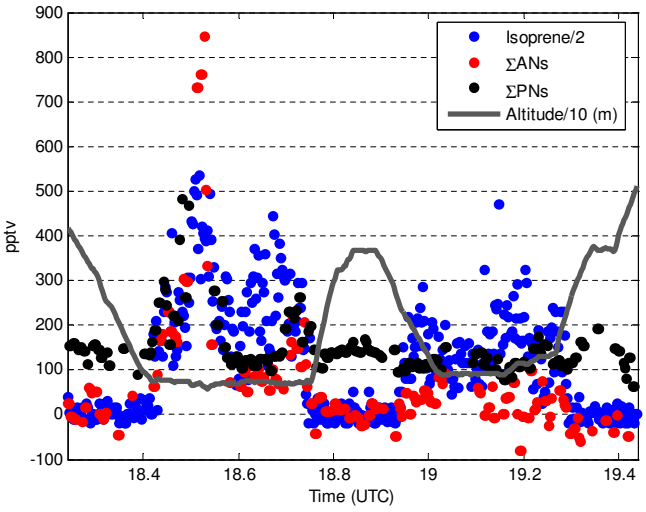

Fig. 1. An example from flight #23 (10 July 2008) of the ΣANs, ΣPNs, and isoprene (from the PTRMS) concentrations versus hour (UTC). The solid line is the altitude of the DC-8 aircraft. The data is from the 10 s merge, version 13.

3 ΣANs concentration and production

In the continental boundary layer over the boreal forest (between 50° and 67.5° N), we observed that ΣANs were 22 % (median) of NO_y (Fig. 2) in background conditions which were sampled on flights 17, 19, 20, and 23. Periods of boundary layer sampling were determined by visually inspecting the potential temperature and ratio of potential temperature to IR surface temperature. The boundary layer heights determined by this method ($\sim$ 1.5–2.4 km a.g.l.) are consistent with boundary layer heights measured over Northern Saskatchewan in July 2002 (Shashkov et al., 2007). The minimum altitude of sampling was just under 500 m. We see no evidence of a significant vertical gradient in the contribution of ΣANs to NO_y, and thus believe the use of the median values to be appropriate. The background conditions were defined to exclude recent anthropogenic and biomass burning influences by only using conditions where CO was less than 180 ppbv and NO_x was less than 200 pptv. Remaining biomass burning influences were removed by visually inspecting the HCN and CH_3CN concentration time series and excluding plumes. The mean concentrations of CO, CH_3CN, and HCN used in our analysis are lower than the means of the background ARCTAS measurements described in Simpson et al. (2011). In this analysis we define NO_y as the sum of the measured individual components of NO_y (NO, NO_2, ΣPNs, ΣANs, gas phase nitric acid, and submicron aerosol nitrate). The observation that ΣANs are on the order of 20 % of NO_y is consistent with almost all past measurements of

Table 1. Species and measurement techniques used in this paper in addition to the core measurement of ΣANs and NO_2.

Species	Method	Reference
VOCs*	Whole air sampling	Blake et al. (2003)
VOCs*	Trace Organic Gas Analyzer (TOGA) Gas chromatography – mass spectrometry	Apel et al. (2003)
VOCs*	Proton transfer reaction mass spectrometry	Wisthaler et al. (2002)
CH_4	Tunable diode laser absorption spectroscopy	Sachse et al. (1987)
NO, O_3	Chemiluminescence	Weinheimer et al. (1994)
OH,HO_2	Laser Induced Fluorescence Chemical ionization mass spectrometry	Faloona et al. (2004); Cantrell et al. (2003); Mauldin III et al. (2003)
HNO_3	Chemical ionization mass spectrometry	Crounse et al. (2006)
Submicron aerosol nitrate, sulphate, ammonium, and organic aerosol	Aerosol mass spectrometry	Cubison et al. (2011)

* A full list of the VOCs from each measurement technique can be found in Appendix A.

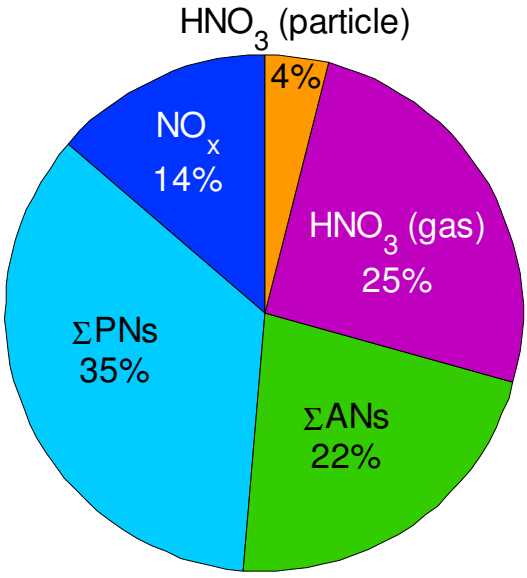

Fig. 2. NO_y composition in the boundary layer over the remote boreal forest for background conditions (see text). HNO_3 (particle) refers to submicron particulate NO_3^- as measured by the AMS and may include a contribution from particulate ΣANs (see text).

ΣANs from TD-LIF in continental locations (Day et al., 2003; Rosen et al., 2004; Cleary et al., 2005; Perring et al., 2009, 2010; Farmer et al., 2011); however, in this data set we find that the instantaneous production rate of ΣANs is larger than the HNO_3 production rate – a situation that has not been reported previously.

Using the measured VOCs, OH, HO_2, and NO concentrations (Table 1), we calculate the instantaneous production rate of ΣANs (P(ΣANs) Eq. 1) via OH oxidation of VOCs by assuming that peroxy radicals are in steady-state (Eqs. 2–3) which results in Eq. (4):

$$P(\Sigma ANs) = \sum_i \alpha_i k_{RO_{2i}+NO}[RO_2]_i[NO], \quad (1)$$

$$\frac{d[RO_2]_i}{dt} = k_{OH+VOCi}[OH][VOC]_i - k_{RO_{2i}+NO}[RO_2]_i[NO] - k_{RO_{2i}+HO_2}[RO_2]_i[HO_2] - \sum_j k_{RO_{2i}+RO_{2j}}[RO_2]_i[RO_2]_j - k_{isom}[RO_2]_i \approx 0, \quad (2)$$

$$[RO_2]_i \approx \frac{k_{OH+VOCi}[OH][VOC]_i}{k_{RO_{2i}+NO}[NO]+k_{RO_{2i}+HO_2}[HO_2]+\sum_j k_{RO_{2i}+RO_{2j}}[RO_2]_j+k_{isom}}, \quad (3)$$

$$P(\Sigma ANs) \approx \sum_i \gamma_i \alpha_i k_{OH+VOCi}[OH][VOC]_i, \quad (4)$$

where

$$\gamma_i = \frac{k_{RO_{2i}+NO}[NO]}{k_{RO_{2i}+NO}[NO]+k_{RO_{2i}+HO_2}[HO_2]+\sum_j k_{RO_{2i}+RO_{2j}}[RO_2]_j+k_{isom}}. \quad (5)$$

Here, k_{isom} refers to the rate of a unimolecular isomerization reaction of RO_2. This class of reactions has recently been shown to be important when the lifetime of RO_2 is long, such as in low NO_x conditions (e.g. Peeters et al., 2009; Peeters and Müller, 2010; Crounse et al., 2011). γ (Eq. 5) represents the fraction of RO_2 that reacts with NO and depends on the identity of the RO_2. We calculate specific γ values for peroxy

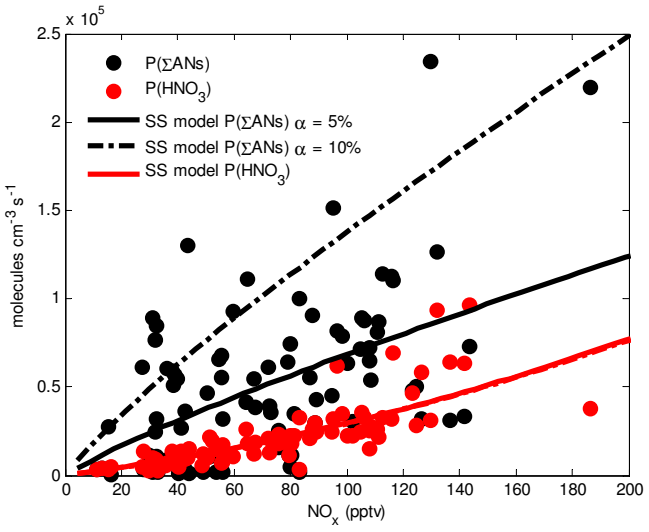

Fig. 3. Calculated instantaneous production rates of HNO_3 (red) and ΣANs (black) as a function of NO_x. The points are calculated using in situ observations as described in Appendix A. The lines are calculations from the steady-state model described in Browne and Cohen (2012). The two black lines shown assume branching ratios of 5 % (solid black line) and 10 % (dashed black line) for ΣANs production from the reaction of RO_2 with NO. These two branching ratios are assumed to bracket the values expected in forested environments.

radicals derived from monoterpenes (α- and β-pinene), isoprene, methacrolein, and methyl vinyl ketone. All other peroxy radicals (which, as shown below, account for only 3 % of the ΣANs production) are assumed to behave like methyl vinyl ketone peroxy radicals. Each of these γ values are calculated using the $RO_2 + HO_2$ rate calculated from the parameterization used in the Master Chemical Mechanism (MCM) v3.2 (Jenkin et al., 1997; Saunders et al., 2003) available at http://mcm.leeds.ac.uk/MCM. We use measured isomerization rates for isoprene peroxy radicals (Crounse et al., 2011) and methacrolein peroxy radicals (Crounse et al., 2012). Although there are theoretical predictions that peroxy radicals derived from monoterpenes undergo a fast ring closure reaction followed by addition of O_2, regenerating a peroxy radical (Vereecken and Peeters, 2004), there are no experimental constraints on the organic nitrate yield for this peroxy radical. We assume that the organic nitrate yield is the same as the parent and thus implicitly assume the isomerization reaction of monoterpene-derived RO_2 is unimportant for our calculation. We also assume that the isomerization reaction is negligible for the remaining RO_2 species. All γ values use the same rate coefficients for $RO_2 + NO$ (from MCM v3.2) and for $RO_2 + RO_2$ (the IUPAC $CH_3O_2 + C_2H_5O_2$ reaction rate available at http://www.iupac-kinetic.ch.cam.ac.uk/, Atkinson et al., 2006). In these calculations, when the measured NO is less than 0 pptv, we assign it a value of 1 pptv. Due to the more complete data coverage, we use the LIF measurements of OH and HO_2; however, the LIF and CIMS data agree well (Ren et al., 2012) and we see no significant difference when using the CIMS data (Appendix A2). Details regarding the VOCs, OH oxidation rates, branching ratios, and uncertainties regarding rate coefficients are described in Appendix A.

The instantaneous production of HNO_3 is calculated using the measured OH and NO_2. We use the rate constant from Mollner et al. (2010) with the temperature dependence from Henderson et al. (2012).

The total calculated P(ΣANs), shown in Fig. 3, is similar to or greater than the calculated nitric acid production. Biogenic species account for the majority (97 %) of P(ΣANs) (Fig. 4) with isoprene (64 %), methyl vinyl ketone (9 %), and α and β-pinene (25 %) contributing the most production. Due to the rapid isomerization of the methacrolein peroxy radical, very few methacrolein nitrates are formed (< 1 % of P(ΣANs)). The conclusion that the P(ΣANs) rate is faster than the P(HNO_3) rate holds for both the isoprene nitrate branching ratio of 11.7 % from Paulot et al. (2009) as shown in Fig. 3 and the lower value of 7 % from Lockwood et al. (2010) (details in Appendix A). The time series of ΣANs and isoprene shown in Fig. 1 illustrates how increases in ΣANs roughly correspond to increases in the precursors (e.g. isoprene).

Since only α and β-pinene were measured aboard the DC-8 aircraft, it is likely that the concentration of monoterpenes is underestimated. Enclosure measurements of black spruce trees (an important constituent of the Canadian boreal forest) indicate that emissions of camphene and 3-carnene are larger than those of α-pinene (Fulton et al., 1998) and extensive measurements of VOCs in the boreal forest of Finland have shown that α- and β-pinene represent only a fraction of the monoterpenes (e.g. Räisänen et al., 2009; Hakola et al., 2012). Vertical profile measurements from the surface to ∼ 800 m in the boreal forest of Finland also indicate steep vertical gradients in monoterpenes and isoprene (Spirig et al., 2004), indicating that production of ΣANs is likely much faster at altitudes lower than those sampled by the DC-8 aircraft (minimum of ∼ 500 m). Since the composition of monoterpenes is dependent on the ecosystem, we do not attempt to scale the monoterpene measurement. Rather, we note that if the monoterpene concentration is doubled, the monoterpene contribution to ΣANs production increases to 39 % reducing the isoprene contribution to 51 %. The median of the ratio of P(ΣANs) to P(HNO_3) also increases from 1.96 to 2.6.

Despite this larger production rate of ΣANs than of HNO_3, the median concentration of ΣANs (108 pptv) is less than the median concentration of the sum of gas phase HNO_3 and particulate NO_3^- (180 pptv). One possible explanation of this apparent discrepancy is that entrainment may have a significant effect on the concentrations. The observed concentration differences during flight segments where the DC-8 crossed the boundary layer indicate that entrainment will

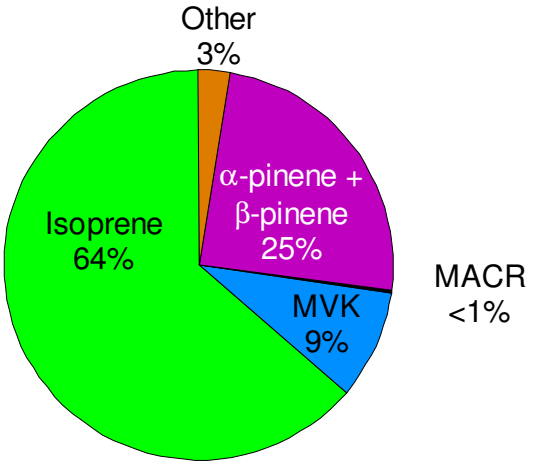

Fig. 4. Distribution of the instantaneous production rate of organic nitrates in the boundary layer over the remote boreal forest. Details of the calculation are described in Appendix A.

dilute both HNO_3 and ΣANs. ΣANs have a slightly faster dilution: the median concentration difference above and within the boundary layer is 1.0×10^9 molecules cm^{-3} for ΣANs and 7.0×10^8 molecules cm^{-3} for HNO_3 (gas + particle). As an upper limit estimate we assume that the average boundary layer height is 1.5 km and is growing at 10 cm s^{-1}. Even with this dilution correction the production rate of ΣANs is greater than that of HNO_3 in 50 % of the boundary layer data. In contrast, in 90 % of the data the concentration of ΣANs is less than that of HNO_3 (gas+particle). Since we use an upper limit estimate of the effect of entrainment and considering the production rate of ΣANs is likely larger than calculated here due to the presence of unmeasured BVOCs (particularly within the forest canopy), we conclude that factors other than entrainment are responsible for the production rate-concentration discrepancy between HNO_3 and ΣANs.

It is also possible that the particulate phase NO_3^- as measured by the aerosol mass spectrometer (AMS) includes a contribution from particle phase ΣANs (e.g. Farmer et al., 2010; Rollins et al., 2010a). For 77 % of the one minute data for which there are both gas phase HNO_3 and ΣANs measurements, the concentration of ΣANs is less than the concentration of gas phase HNO_3. Therefore, the possible contribution from ΣANs to the AMS NO_3^- signal does not affect our conclusions that HNO_3 is generally present in higher concentrations than ΣANs. In the remainder of the manuscript HNO_3 will refer to the sum of gas phase HNO_3 and particulate NO_3^- unless stated otherwise.

We conclude that the larger production rate yet smaller concentration of ΣANs than of HNO_3 implies a shorter lifetime of ΣANs than of HNO_3. We note that the lifetime of ΣANs represents the loss of the nitrate functionality and thus will be longer than the average lifetime of individual nitrates because oxidation of some nitrates results in products that are more highly functionalized ANs.

4 Lifetime of HNO_3

The lifetime of HNO_3 in the boundary layer is primarily determined by deposition that, for gas phase HNO_3, is generally assumed to occur with unit efficiency at a mass transfer rate set by turbulence. Assuming an approximate boundary layer height of $\sim$ 2 km (we observed boundary layer heights that ranged from 1.5 km to 2.6 km) and a deposition velocity of 4 cm s^{-1}, we calculate a lifetime of $\sim$ 14 h (loss rate of 2×10^{-5} s^{-1}) for HNO_3 for midday conditions. The deposition velocity of HNO_3 over forests has been reported to range from 2 cm s^{-1} to 10 cm s^{-1} (Horii et al., 2005 and references therein), with a strong variation associated with time of day and season. Given the uncertainty and time of day dependence also associated with the boundary layer height, we use this lifetime as a guide for thinking about the daytime lifetime of ΣANs, which our measurements indicate is shorter than that of HNO_3, and do not focus on the exact number. The depositional loss of aerosol phase NO_3^- is generally on the order of days, however, due to its low contribution to total HNO_3 (Fig. 2), we consider only the gas-phase loss. Other losses, photolysis and oxidation by OH, are quite slow with median lifetimes of several weeks.

5 Lifetime of ΣANs

Using the ARCTAS data we are unable to constrain the exact ΣANs lifetime since to do so would require knowledge of the photochemical age of the air mass, the history of ΣANs production (which is likely to have significant vertical gradients), and the exact chemical speciation of the ΣANs. However, with the constraint imposed by the HNO_3 data and with some reasonable assumptions we can identify the most likely ΣANs loss processes.

5.1 Deposition

Deposition is likely a significant term in the ΣANs budget, however, the deposition velocity of ΣANs will be less than that of HNO_3. The measured Henry's law coefficients of some of the more soluble individual hydroxy nitrates ($\sim 10^3$–10^5 M atm^{-1}, Shepson et al., 1996; Treves et al., 2000) are orders of magnitude lower than that of HNO_3 (1×10^{14} M atm^{-1} at pH $\sim$ 6.5, Seinfeld and Pandis, 2006). Still, these measured Henry's law coefficients of hydroxy nitrates indicate that wet deposition is a significant loss process and a recent study indicates that foliar uptake of organic nitrates is possible (Lockwood et al., 2008). The only direct simultaneous measurements of ΣANs and HNO_3 deposition are those of Farmer and Cohen (2008) who estimated a ΣANs dry deposition velocity of 2.7 cm s^{-1} compared to

$3.4\,cm\,s^{-1}$ for HNO_3 above a ponderosa pine forest. Similar results have been obtained more recently at the same forest (K.-E. Min, personal communication, 2012). Although the exact magnitude of the depositional loss likely depends on the specific composition of ΣANs, as well as the partitioning between gas and aerosol, we assume that a similar result exists for the boreal forest since recent measurements of speciated organic nitrates using chemical ionization mass spectrometry at the ponderosa pine forest (Beaver et al., 2012) indicate a similar composition of ΣANs as assumed here from the instantaneous production rate. Therefore, although the deposition of ΣANs is important, it is slower than the deposition of HNO_3, thus implying the existence of other sinks of ΣANs. In other words, chemistry must be an important sink of ΣANs.

5.2 Photolysis

The OH oxidation of both isoprene and monoterpenes produces hydroxy nitrates as first generation products. These molecules account for at least 89 % of the instantaneous production rate of ΣANs (Fig. 4) for the conditions considered here. Although there are no direct measurements of the photolysis rates of these specific molecules, by analogy to other compounds we estimate that photolysis is a negligible sink for them. Roberts and Fajer (1989) report that the cross section of nitrooxy ethanol is approximately a factor of three smaller than methyl nitrate. Similarly, photolysis rates of alkyl nitrates are on the order of several days (e.g. Roberts and Fajer, 1989; Talukdar et al., 1997) and are thus too slow to be important. In contrast, α-nitrooxy ketones have been shown to have a cross section approximately five times larger than alkyl nitrates (Roberts and Fajer, 1989; Barnes et al., 1993). Our calculations suggest these are too small a fraction of the total to affect the overall lifetime. To estimate an upper limit, we use the fastest reported photolysis rate from Suarez-Bertoa et al. (2012), which is for 3-methyl-3-nitrooxy-2-butanone. This rate was calculated assuming solar conditions appropriate for 1 July at noon at 40° N. To achieve a rate appropriate for the ARCTAS conditions we use the median rates of methyl and ethyl nitrate photolysis measured during ARCTAS and scale these to the rate of 3-methyl-3-nitrooxy-2-butanone using the measurements of Roberts and Fajer (1989) and Suarez-Bertoa et al. (2012). We take the average of the rate calculated from methyl nitrate and from ethyl nitrate and assume that 9 % of the nitrates (the methyl vinyl ketone contribution in Fig. 4) are α-nitrooxy ketones. This results in an overall photolysis rate for ΣANs of $2.5 \times 10^{-6}\,s^{-1}$ (lifetime of $\sim 110\,h$), a rate that even when combined with deposition is too slow to account for the inferred ΣANs loss.

5.3 Oxidation

The overall gas-phase chemical removal rate of ΣANs can be represented as

$$k_{\text{ox-loss}} = \sum_i k_{\text{AN}_i+\text{OX}}[\text{OX}]\frac{[\text{AN}_i]}{[\Sigma\text{ANs}]}\chi_i, \quad (6)$$

where $k_{\text{AN}i+\text{OX}}$ the rate constant of that oxidant with the specific nitrate, [OX] represents the concentration of oxidant (OH, O_3, or NO_3), $[\text{AN}_i]$ represents the concentration of a specific nitrate, and χ_i the fraction of the reaction that results in loss of the nitrate functionality (referred to as NO_x recycling). To simplify our calculation, we neglect the possibility that the oxidation of nitrates results in the formation of dinitrates which would result in a small positive term in Eq. (6). We also ignore oxidation by NO_3 since we only use daytime measurements above the forest canopy.

We estimate the composition of ΣANs as a mixture of the small, long-lived, alkyl nitrates measured in the whole air samples (which account for a median of 30 % of the ΣANs measured by TD-LIF) and molecules that can be estimated from the instantaneous production rate of ΣANs (Fig. 4). The small nitrates have very long lifetimes and are a negligible term in the overall loss rate. We use the OH oxidation rates of isoprene-derived nitrates (assuming 60 % δ-hydroxy isoprene nitrates and 40 % β-hydroxy isoprene nitrates) and methyl vinyl ketone-derived nitrates from Paulot et al. (2009). Recently, Lockwood et al. (2010) have measured the ozone oxidation rate of three of the eight possible isoprene nitrate isomers. The three isomers include one δ-hydroxy isomer and two β-hydroxy isomers. We assume that the δ-hydroxy isoprene nitrate rate constant from Lockwood et al. (2010) is representative of all δ-hydroxy isomers. The rate constants for two β-hydroxy isomers differ by approximately a factor of three and we bound the possible range of reaction rates using these two rates. This results in an ozonolysis rate ranging from $7.4 \times 10^{-17}\,cm^3\,molecules^{-1}\,s^{-1}$ to $1.7 \times 10^{-16}\,cm^3\,molecules^{-1}\,s^{-1}$. Results using the branching ratio between the δ and β-hydroxy nitrate channels as determined by Lockwood et al. (2010) (and updated by Pratt et al., 2012) are included in Appendix B.

We are unaware of any experimental constraints on the oxidation rate of monoterpene nitrates by OH and we estimate an OH oxidation rate constant of $4.8 \times 10^{-12}\,cm^3\,molecules^{-1}\,s^{-1}$ based on a weighting of the MCM v3.2 rates for α-pinene and β-pinene nitrates as described in Browne et al. (2013). The monoterpene nitrates in our calculations are based on the production from the observed concentrations of α- and β-pinene, the only two monoterpenes measured aboard the aircraft. These nitrates will predominantly be saturated molecules and thus ozonolysis of these nitrates should be too slow to be important. As discussed in Sect. 3, it is likely that the contribution of monoterpene nitrates is underestimated. It is therefore possible that some of the monoterpene-derived nitrates may be

Table 2. Median oxidation rates calculated using the assumptions from the text. Here k_{AN+OX} refers to the rate of reaction with the class of organic nitrates with either OH or O_3, β and δ refer to the NO_x recycling following reaction with OH or O_3, respectively, and $(1-F_{RO_2+HO_2})$ refers to the fraction of RO_2 reactions that lead to NO_x recycling (i.e. the fraction of the time RO_2 reacts with either NO or other RO_2). The two numbers listed for the isoprene + O_3 rate reflect the range in possible β-hydroxy isoprene nitrate ozonolysis rates.

ΣAN precursor	k_{AN+OX} [OX]	$[AN_i]/[\Sigma ANs]$	β or δ	$(1-F_{RO_2+HO_2})$	Loss rate (s^{-1})
Isoprene	6.2×10^{-11} [OH]	0.45	0.55	0.27	4.3×10^{-6}
Isoprene	1.7×10^{-16} [O_3] (7.4×10^{-17} [O_3])	0.45	0.40	N/A	2.5×10^{-5} (1.1×10^{-5})
MVK	0.56×10^{-11} [OH]	0.06	1	0.29	1.1×10^{-7}
Monoterpenes	4.8×10^{-12} [OH]	0.18	1	0.22	2.0×10^{-7}
				Total	3.1×10^{-5} (1.5×10^{-5})

unsaturated molecules. We discuss the impact of this possibility in Appendix B and conclude that since the release of NO_2 from these molecules following oxidation is likely low, the effect on the oxidation rate is minimal.

The NO_x recycling (χ) following OH oxidation depends on the fate of the resulting nitrooxy peroxy radical ($R(NO_3)O_2$) which may react with NO, HO_2, or other RO_2. We assume that reactions with HO_2 generate a more highly functionalized nitrate and that the NO_x recycling (the loss of the nitrate functionality) occurs with the same efficiency through both the $R(NO_3)O_2 + NO$ and $R(NO_3)O_2 + RO_2$ channels. We use the same assumptions for the $R(NO_3)O_2 + HO_2$ rate as in the calculation of γ in Sect. 3, however, we assume that no isomerization reactions occur. We find that $RO_2 + RO_2$ reactions account for at most 1 % of the RO_2 reactions. Uncertainties regarding these estimations are discussed in Appendix B. NO_x recycling from the $RO_2 + NO$ reaction have been constrained by laboratory experiments to be $\sim$ 55 % for isoprene nitrates and 100 % for MVK nitrates (Paulot et al., 2009). We are unaware of any measurements of NO_x recycling from monoterpene nitrates and assume a value of 100 % as an upper limit. Although the molecular structure of monoterpene nitrates implies that the NO_x recycling is likely much lower than 100 %, the contribution (as calculated below) from monoterpene nitrates to NO_x recycling is negligible making a more accurate estimate unnecessary.

NO_x recycling following ozonolysis of unsaturated nitrates (isoprene nitrates) depends on the initial branching of the ozonide to the two possible pairs of a carbonyl molecule and an energy-rich Criegee biradical and the subsequent fate of the Criegee biradical (stabilization or decomposition). To our knowledge, no experimental constraints on this process exist for any unsaturated organic nitrate. The MCM v3.2 assumes equal branching between the two possible carbonyl/Criegee biradical pairs; we calculate NO_x recycling (40 %) using the MCM v3.2 products of the ozonolysis of isoprene nitrates, the assumption that a stabilized Criegee biradical reacts only with water, and the relative abundances of the different isoprene nitrate isomers from Paulot et al. (2009) (ignoring the minor 3,4 and 2,1 isomers). Using the relative abundances of the different isoprene nitrate isomers from Lockwood et al. (2010) (updated with the numbers from Pratt et al., 2012) results in a NO_x recycling of 38 %.

Our calculation of the ΣANs loss rate can be summarized by expanding Eq. (6) to

$$k_{\text{ox-loss}} = \sum_i k_{AN_i+OH}[OH]\frac{[AN_i]}{[\Sigma ANs]}\beta_i(1-F_{RO_{2i}+HO_2}) + \sum_i k_{AN_i+O_3}[O_3]\frac{[AN_i]}{[\Sigma ANs]}\delta_i, \quad (7)$$

$$F_{RO_2+HO_2} = \frac{k_{RO_{2i}+HO_2}[HO_2]}{k_{RO_{2i}+NO}[NO] + k_{RO_{2i}+HO_2}[HO_2] + \sum_j k_{RO_{2i}+RO_{2j}}[RO_{2j}]}. \quad (8)$$

Here, β represents the fraction of NO_x recycled following the reaction of the peroxy radical with RO_2 or NO, $F_{RO_2+HO_2}$ (Eq. 8) represents the fraction of the time that the peroxy radical reacts with HO_2 (and thus does not recycle NO_x), and δ represents the NO_x recycling from ozonolysis. Uncertainties regarding this calculation are described in Appendix B.

Using the assumptions above, we calculate a chemical ΣANs lifetime of $\sim$ 9–18 h (Table 2) which ranges from slightly shorter to slightly longer than our estimated HNO_3 lifetime ($\sim$ 14 h). In combination with deposition ($\sim$ 17.5 h for a 2 km boundary layer), a detailed representation of oxidative ΣANs loss results in a calculated ΣANs lifetime in the range of the assumed lifetime of HNO_3. In these calculations, the majority of ΣANs loss occurs via isoprene nitrate ozonolysis, which has recently been reported to be much faster than previously assumed (Lockwood et al., 2010). Additional measurements of this rate and the products are important to constraining our understanding of ΣANs and their role in the NO_x budget.

5.4 Hydrolysis of particulate organic nitrates

5.4.1 Loss of ΣANs

Although we calculate a ΣANs loss rate due to oxidation and deposition that is similar to the assumed loss rate of HNO_3, the recent suggestion that organic nitrates may undergo hydrolysis in aerosols to produce HNO_3 as a product (Sato, 2008; Darer et al., 2011; Hu et al., 2011) is also a viable hypothesis to explain the measurements. Evidence for organic nitrate losses in ambient (Day et al., 2010) and chamber generated particles (Liu et al., 2012) analyzed with IR spectroscopy is consistent with this mechanism. This chemistry results in the depletion of ΣANs and an enhancement in HNO_3; both effects would contribute to the ratio of ΣANs to HNO_3 production and concentration that we report here.

Bulk solution studies of hydrolysis of organic nitrates indicate that primary and secondary nitrates are stable at atmospherically relevant pH, but that the lifetime of tertiary hydroxy organic nitrates is surprisingly short (0.019–0.67 h), even in neutral solutions (Darer et al., 2011; Hu et al., 2011). Since these are bulk solution studies, there are some difficulties associated with extending the rates to aerosol processes. Namely, the question arises as to whether the nitrates are present in the organic or aqueous phase of the aerosol and if the availability of liquid water is sufficient for the reaction. Some of these issues have been recently discussed by Liu et al. (2012) who, using a smog chamber without seed aerosol, constrained the hydrolysis of particulate organic nitrates derived from the photo oxidation of 1,2,4-trimethylbenzene. Using their measurements of the organic aerosol composition, they calculated a lifetime of ~ 6 h for particulate organic nitrates when the relative humidity was greater than 20 %.

Since the vapor pressures of first generation isoprene nitrates are generally too high to partition into aerosol (Rollins et al., 2009), we begin the estimation of the hydrolysis rate by assuming that only monoterpene nitrates are present in organic aerosol. Although Henry's law coefficients of small ($\leq$ 5 carbons) hydroxy nitrates have been measured to be quite large, approximately $\sim 10^3$–10^5 M atm^{-1} (Shepson et al., 1996; Treves et al., 2000), it is reasonable to assume that as a ten carbon compound, a monoterpene nitrate may have a lower Henry's law coefficient. We therefore assume that these nitrates partition only into organic aerosol and that the organic aerosol contains sufficient liquid water for this reaction to occur (median RH of 63 % and minimum of 34 %).

We use absorptive partitioning theory to determine the fraction of the monoterpene nitrate in the particle phase (Pankow, 1994; Donahue et al., 2006):

$$C_i^* = \frac{C_i^{\mathrm{g}} C_{\mathrm{OA}}}{C_i^{\mathrm{a}}} = \frac{\mathrm{MW}_i \cdot 10^6 \cdot \zeta_i \cdot p_i}{760 \cdot R \cdot T}. \quad (9)$$

Here C_i^* represents the effective saturation concentration ($\mu g\,m^{-3}$) of the organic nitrate, C_i^{a} is the concentration of the organic nitrate in the condensed phase ($\mu g\,m^{-3}$), $C_{\mathrm{i}}^{\mathrm{g}}$ the concentration of the organic nitrate in the gas phase ($\mu g\,m^{-3}$), and C_{OA} is the concentration of organic aerosol ($\mu g\,m^{-3}$). In the second equality R is the universal gas constant (8.206×10^{-5} atm m^3 K^{-1} mol^{-1}), MW_i is the molecular weight of the organic nitrate (assumed here to be a hydroxy monoterpene nitrate – 215 g mol^{-1}), ζ_i is the molality based activity coefficient (assumed to be 1), p_i is the vapor pressure of the organic nitrate (Torr), and 760 and 10^6 are unit conversion factors. We calculate an estimated bound on the partitioning of monoterpene nitrates to the aerosol using vapor pressures of 4×10^{-6} Torr ($C_i^* =$ of 48 $\mu g\,m^{-3}$ at 286 K – the median temperature during ARCTAS) derived from chamber measurements of nitrate products of the $NO_3 + \beta$-pinene reaction (Fry et al., 2009) and of 5.8×10^{-7} Torr ($C_i^* = 7\,\mu g\,m^{-3}$) from chamber measurements of the $NO_3 +$ limonene reaction (Fry et al., 2011). The organic aerosol loading is from the AMS measurement and can be subdivide into two distinct regimes: one with a median loading of $\sim 1\,\mu g\,m^{-3}$ (at ambient temperature and pressure) and one with a median loading of $\sim 6.6\,\mu g\,m^{-3}$. The enhanced loading regime (60 % of the data) was associated with higher concentrations of acetone, a known oxidation product of monoterpenes, suggesting that monoterpenes are an important source of SOA. This is consistent with measurements in southern Ontario reporting high concentrations of biogenic SOA (Slowik et al., 2010). The concentration of the biogenic species (α-pinene, β-pinene, isoprene, MVK, and MACR) were all higher in the regime of enhanced organic aerosol loading than in the lower loading regime. The isoprene oxidation products showed higher enhancements (e.g. 181 % equivalent to 278 pptv for MVK) than did isoprene (18 %–53 pptv). The concentration enhancement of acetone (117 %–1.23 ppbv) was also larger than that of the monoterpenes (105 %–122 pptv), however, the long lifetime and multiple sources of acetone make a direct attribution to monoterpene oxidation impossible. Nevertheless, it is clear that the enhanced loading regime represents a larger biogenic influence and is more aged than the lower loading regime.

The fraction of the monoterpene nitrate in the aerosol (F_{aero}) is calculated using Eq. (10).

$$F_{\mathrm{aero}} = \frac{C_i^{\mathrm{a}}}{C_i^{\mathrm{a}} + C_i^{\mathrm{g}}} = \left(1 + \frac{C_i^*}{C_{\mathrm{OA}}}\right)^{-1} \quad (10)$$

We calculate the loss rate of ΣANs through hydrolysis ($k_{\mathrm{hyd\text{-}loss}}$) using Eq. (11):

$$k_{\mathrm{hyd\text{-}loss}} = \sum_i k_{\mathrm{hyd}} F_{\mathrm{aero},i} F_{\mathrm{tertiary},i} \frac{[\mathrm{AN}_i]}{[\Sigma\mathrm{ANs}]}, \quad (11)$$

where F_{tertiary} represents the fraction that is tertiary nitrate and k_{hyd} represents the hydrolysis rate constant. We set F_{tertiary} at 75 %, midway between the 63 % for α-pinene nitrates and 92 % for β-pinene nitrates from MCM v3.2. We

Table 3. Median calculated loss rate of ΣANs due to hydrolysis in the particle phase assuming that only monoterpene nitrates may partition into the aerosol and hydrolyze. We consider cases that span different vapor pressures, hydrolysis rates, and organic aerosol loadings. Here, C^* represents the effective saturation concentration, τ_{hyd} is the lifetime to hydrolysis for a tertiary nitrate in the particle phase, $k_{hyd\text{-}loss}$ is the calculated loss rate of ΣANs via hydrolysis (see text for details), and the last column is the median of the ratio of this HNO_3 source to the source from the reaction of OH with NO_2. After correction for the small alkyl nitrates, monoterpenes accounted for ∼ 10 % (∼ 19 %) (median value) of the ΣANs in the low (high) aerosol loading periods. We assume that only a fraction (75 %) of the monoterpene nitrates undergo hydrolysis and thus the fraction of the ΣANs that are in the particle phase and undergoing hydrolysis is 2–7 % for the high loadings and < 1 % for the low loadings.

Organic aerosol loading (μg^{-3})	C^* (μg^{-3})	τ_{hyd} (h)	$k_{hyd\text{-}loss}$ (s^{-1})	$k_{hyd\text{-}loss}$ [ΣANs]/ (k_{OH+NO_2} [OH][NO_2])
1	7	6	3.8×10^{-7}	0.03
6.6	7	6	3.2×10^{-6}	0.53
1	48	6	6.1×10^{-8}	0.00
6.6	48	6	8.0×10^{-7}	0.13
1	48	0.67	5.5×10^{-7}	0.04
6.6	48	0.67	7.2×10^{-6}	1.16

note that the fraction of ΣANs predicted to be derived from monoterpenes based on the instantaneous production rate changes insignificantly between the low and enhanced loadings and we use the value from Fig. 4. However, in the low loading regime the small alkyl nitrates represent a larger fraction of ΣANs (61 %) than in the enhanced loading regime (23 %). Thus, the absolute fraction of ΣANs from monoterpene nitrates is higher in the enhanced loading regime.

Based on the work by Elrod and co-workers (Darer et al., 2011; Hu et al., 2011) showing an order of magnitude variation in the tertiary nitrate hydrolysis lifetime, it appears that the identity of the organic nitrate influences the hydrolysis rate. Although these bulk solution rates may not be strictly applicable to aerosol processes, it is also likely that the lifetime reported by Liu et al. (2012) for 1,2,4 – trimethylbenzene-derived organic nitrates may not apply to biogenic systems. Therefore, we calculate the overall ΣANs hydrolysis rate ($k_{hyd\text{-}loss}$) for three different combinations of hydrolysis rates (k_{hyd}) and C^* values as shown in Table 3.

In the enhanced loading regime these rates range from 2 % to 20 % of the oxidative lifetime (assuming the faster ozonolysis rate). It should be emphasized that the hydrolysis loss rate calculated here is reflective of the hydrolysis loss rate averaged over all the individual organic nitrates; in other words, the loss rate of an individual nitrate might be faster or slower than this rate. In fact, the rate calculated here is the result of only ∼ 2 % ($C^* = 48\,\mu g\,m^{-3}$) or ∼ 7 % ($C^* = 7\,\mu g\,m^{-3}$) of the ΣANs undergoing hydrolysis in the enhanced loading regime and for < 1 % of the ΣANs (regardless of C^* value) undergoing hydrolysis in the low loading regime. Any changes to this fraction will result in proportional changes to the overall hydrolysis rate. Consequently, due to the chemical complexity of this process our range of rates should not be taken as upper and lower estimates of the impact of this channel. Rather, this range should be interpreted as evidence that the hydrolysis reaction may represent an important, previously unaccounted for ΣANs loss process as well as a potentially important source of HNO_3. This loss process of ΣANs is important in that unlike the oxidative pathway, hydrolysis represents a sink of ΣANs that removes NO_x from the atmosphere.

5.4.2 Production of HNO_3

In addition to being a sink of ΣANs the hydrolysis reaction may also be an important source of HNO_3. As shown in Table 3, the ratio of this HNO_3 source to the known source from the reaction of OH with NO_2 and ranges from a median of 0.13 to greater than 1 in the enhanced loading regime. We believe that this upper limit is likely incompatible with the HNO_3 budget and is likely the result of extrapolating bulk solution rates to aerosol environments; however, we do find evidence of this HNO_3 source in the variation of the ratio of HNO_3 to NO_2 with NO_x. In the boundary layer when the lifetime of HNO_3 is short, HNO_3 is in photochemical steady-state and the ratio of HNO_3 to NO_2 should be proportional to the OH concentration (Day et al., 2008). We estimate the lifetime of HNO_3 to be ∼ 14 h, a value short enough that HNO_3 should be in diurnal steady-state. When there is a substantial concentration of ΣANs, the ratio of HNO_3 to NO_2 increases while NO_x decreases. OH, however, exhibits the opposite trend and it decreases (Fig. 5a). For conditions of low ΣANs, the ratio of HNO_3 to NO_2 is more similar to OH. It is unlikely that variations in photochemical age are the dominant factor explaining the observed behavior of the HNO_3 to NO_2 ratio (Fig. 5a). The largest deviation in the expected behavior of the HNO_3 to NO_2 ratio as a function of NO_x occurs at the lowest NO_x concentrations – air masses which are likely to be more aged than those with higher NO_x concentrations. However, the deviation only occurs in those air masses with a substantial concentration of both ΣANs (Fig. 5a) and monoterpenes (not shown) and thus likely higher aerosol phase organic nitrates. Other than NO_x concentration, other available chemical tracers for defining age with time zero at biogenic emissions were found to be unsuitable because of their direct correlations with ΣANs or because their sources were not unique.

This trend of increasing values as NO_x decreases is also the same trend as the ratio of P(ΣANs) to P(HNO_3) (where P(HNO_3) = k_{OH+NO_2}[OH][NO_2]) as shown in Fig. 5b using results from the steady-state model in Browne and Cohen (2012). The similarity in magnitude between the HNO_3 to NO_2 ratio and the P(ΣANs) to P(HNO_3) ratio is expected if the hydrolysis of ΣANs constitutes the major loss process

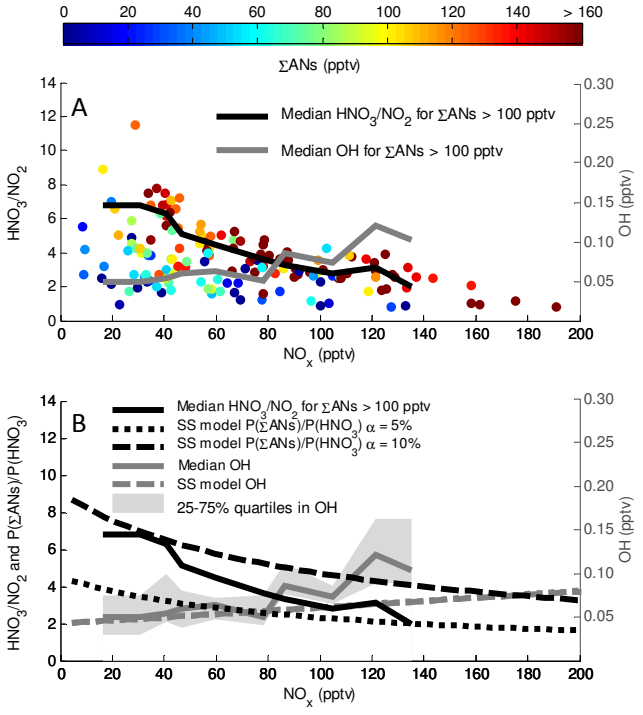

Fig. 5. (A) On the left y-axis is the ratio of HNO_3 (gas+particle) to NO_2 versus NO_x colored by ΣANs concentration. The solid lines are binned median values of points corresponding to ΣANs concentrations ≥ 100 pptv (55 % of the data) for the ratio of HNO_3 to NO_2 (black line, left y-axis) and for OH concentration (grey line, right y-axis). If HNO_3 is in steady-state the ratio of HNO_3 to NO_2 should be equivalent to OH. The difference in these two lines as a function of NOx indicates the possibility of additional HNO_3 sources. **(B)** Comparison between the ARCTAS measurements and predictions from the steady-state model described in Browne and Cohen (2012). The solid lines are the same as in Fig. 5a with the shaded grey area representing the interquartile range of the OH concentration. The dashed and dotted black lines represent the steady- state model predictions of the ratio of ΣANs production to HNO_3 production for branching ratios of 10 % and 5 % respectively (left y-axis). The dashed grey line represents the steady-state model prediction of the OH concentration (right y-axis).

of ΣANs (i.e. that the ratio of hydrolysis to oxidation may be higher than our calculations here suggest). These results suggest that the ARCTAS HNO_3 concentration is consistent with a source of HNO_3 other than the reaction of OH with NO_2 and that this source is likely the hydrolysis of ΣANs.

There are similar hints of this additional HNO_3 source in a reinterpretation of data from previous experiments. Previous measurements of HNO_3 have found evidence for a temperature dependent OH source (Day et al., 2008) and of an elevated within canopy OH concentration (Farmer and Cohen, 2008) in a ponderosa pine forest. However, these results are also consistent with a source of HNO_3 from rapid ΣANs hydrolysis. For instance, the temperature dependent OH source may result from an increase in biogenic VOC emissions with temperature resulting in a larger ΣANs production and consequently a larger HNO_3 source. Likewise, the rapid hydrolysis of ΣANs with low vapor pressures formed from sesquiterpenes and monoterpenes in the forest canopy would result in a within canopy source of HNO_3. This reinterpretation of the HNO_3 data as resulting from an additional production pathway (via hydrolysis of ΣANs) rather than through an elevated concentration of OH is also more consistent with OH measurements made in the same forest a few years later (Mao et al., 2012) that report a within-canopy OH gradient and temperature dependence smaller than that inferred from the previous studies. However, we note that these studies were conducted in different years and it is possible that the ecosystem and its within-canopy chemistry have changed in between those years.

It is interesting to consider the ultimate fate of the NO_3^- possibly produced by the organic nitrate hydrolysis. In 57 % of the background measurements the molar ratio of sulfate to ammonium (as measured by the AMS) is greater than one-half, indicating that it is unfavorable for NO_3^- to be present in the aerosol and that ΣANs hydrolysis is possibly a source of gas phase HNO_3. However, this is a simplistic approximation to an extremely complex problem. The thermodynamics of an aerosol that is an organic-inorganic mixture are much more complex (Zuend et al., 2011) than purely inorganic aerosols and are subject to uncertainties regarding the composition of aerosol and the interaction of ions with various functional groups present on organic species. Further studies on organic nitrate hydrolysis in aerosols are needed to better constrain the atmospheric impacts; however, it appears that the hydrolysis of organic nitrates may contribute (quite significantly) to HNO_3 production.

These results suggest the need for research constraining the possible hydrolysis loss of ΣANs and the associated HNO_3 production. In particular, we need measurements of how the hydrolysis of organic nitrates from biogenic species differs in aerosol versus bulk solution, the aerosol liquid water content necessary for this reaction, and specific rates for monoterpene nitrates.

6 Implications

As shown in Fig. 3, the calculated ΣANs production for most of the data is similar to the steady-state model results from Browne and Cohen (2012) if we assume a branching ratio somewhere between 5 % and 10 % for ΣANs formation from the entire VOC mixture. For the ARCTAS data we calculate that the biogenic VOCs account for ∼ 53 % of the VOC reactivity with respect to OH (median value not including CO and CH_4). Assuming that the biogenic VOCs are the only sources of ΣANs with an average branching ratio of 11 % (similar to isoprene), results in an overall branching ratio of ∼ 6 %. This suggests that the NO_x lifetime and ozone production efficiency in the boreal forest are similar to those calculated in

Browne and Cohen (2012) and that the steady-state model provides a useful framework for understanding the NO_x budget under low NO_x conditions on the continents.

However, as discussed in Browne and Cohen (2012), the net regional and global impact of ΣANs on NO_x lifetime and ozone production depends on the degree to which ΣANs serve as a permanent versus temporary NO_x sink. Modeling studies have found that different assumptions regarding NO_x recycling from isoprene nitrates result in large sensitivities in NO_x and O_3 (e.g. von Kuhlmann et al., 2004; Paulot et al., 2012; Fiore et al., 2005; Horowitz et al., 2007; Wu et al., 2007) and that these uncertainties affect predictions of ozone in a future climate (e.g. Ito et al., 2009; Weaver et al., 2009). The analysis presented here suggests that ΣANs have a short atmospheric lifetime due to a combination of deposition and chemical loss, but we find the data is ambiguous about the relative fraction of the ΣANs chemical loss that acts to release NO_x or to produce HNO_3. Furthermore, the exact fate of ΣANs loss is likely ecosystem dependent; for instance, ΣANs may have a significantly different impact on the NO_x budget in forests dominated by isoprene emissions versus in forests dominated by monoterpene emissions since first generation monoterpene nitrates have lower vapor pressures than first generation isoprene nitrates.

Due to the lumped treatment of ΣANs in most condensed chemical mechanisms, it is likely that these mechanisms will be unable to reproduce the ARCTAS results, and consequently are misrepresenting the NO_x lifetime and ozone production. For instance, some condensed mechanisms instantaneously convert isoprene nitrates to HNO_3, resulting in zero NO_x recycling. The ozonolysis of isoprene nitrates is also ignored in many mechanisms; this is incompatible with our results that the majority of NO_x recycling during ARCTAS results from ozonolysis. Lastly, many condensed mechanisms ignore monoterpene nitrates or lump them into a long-lived nitrate. Our results suggest that, at least in the boreal forest, monoterpene nitrates are an important NO_x sink and that their particle phase hydrolysis may represent a source of HNO_3.

Finally, it is interesting to note that since the loss of ΣANs through hydrolysis depends on the specific isomer of the nitrate, there are interesting implications for the loss of monoterpene nitrates formed from OH versus from NO_3 chemistry. Based on the assumption that tertiary radicals are more stable than primary radicals and thus have a higher nitrate yield, the oxidation of α- or β-pinene and limonene by NO_3 is more likely to result in a primary nitrate and oxidation by OH is more likely to result in a tertiary nitrate. Thus, nitrates formed by OH oxidation may have a shorter atmospheric lifetime than those formed from NO_3 chemistry.

7 Conclusions

We present the first measurements of ΣANs over the remote boreal forest of Canada and show that ΣANs are present in significant concentrations. Using measurements of VOCs we calculate the instantaneous production rate of ΣANs and find that, as expected for a remote forested environment, biogenic species, specifically monoterpenes and isoprene, dominate the ΣANs production. If the observations of α- and β-pinene underestimate the total source of monoterpenes then monoterpenes play an even larger role, than the 25 % we calculate. We also find that the instantaneous production rate of ΣANs is, in general, faster than that of gas phase HNO_3 production, despite a lower overall concentration, implying that ΣANs have a shorter lifetime than HNO_3. We estimate that depositional loss of ΣANs is important and that the combined loss to reaction with O_3 and OH occurs at a rate similar to the assumed deposition rate of HNO_3. Oxidation of isoprene nitrates, in particular by O_3, is primarily responsible for the rapid loss rate. We emphasize that this oxidative loss rate represents the loss of the nitrate functionality and that oxidative reactions of individual nitrates are faster since some of their products are more highly functionalized nitrates.

We also provide evidence which suggests that particulate organic nitrates undergo rapid hydrolysis contributing to HNO_3 production. Although, we are unable to constrain the magnitude of this source precisely, all reasonable assumptions imply that it is significant both as a loss of ΣANs and is a source of HNO_3. Furthermore, there is evidence of its existence in the variation of the HNO_3 to NO_2 ratio as a function of NO_x. We conclude that the rapid loss of ΣANs required to explain these observations is a balance between processes which recycle NO_x (oxidation) and those which remove it (hydrolysis and deposition).

Appendix A

A1 Calculation of ΣANs production

In the calculation of the ΣANs production rate we use the VOCs, branching ratios, and OH reaction rates listed in Table A1. We do not attempt to estimate the concentration of any unmeasured VOCs or to fill in any missing data.

A2 Uncertainties in the calculation of ΣANs production

The calculated production of ΣANs is sensitive to the assumptions about reaction rates, organic nitrate branching ratios, the assumption that the VOC measurements are representative of the entire VOC mix, and possible errors in measurements. We have investigated several possibilities (outlined in Table A2) and find that our conclusion is robust. In Table A2 we show the median value of the ratio of the

Table A1. VOC parameters used in the calculation of the instantaneous production rate of ΣANs.

VOC	α	OH reaction rate	VOC	α	OH reaction rate
Alkanes			Alkenes		
methane[a]	0.001[e]	2.45E-12 × exp(−1775/T)[k]	ethene[b]	0.0086[h]	$k_o = 1.0\text{E-}28 \times (T/300)^{-4.5}$ $k_\infty = 7.5\text{E-}12 \times (T/300)^{-0.85}$ $F_c = 0.6$ $N = 1$[k, r]
ethane[b]	0.009[e]	7.66E-12 × exp(−1020/T)[k]	propene[b]	0.015[h]	$k_o = 8\text{E-}27 \times (T/300)^{-3.5}$ $k_\infty = 3.0\text{E-}11 \times (T/300)^{-1}$ $F = 0.5$ $N = 0.75 - 1.27 \times \log(F_c)$[l, r]
propane[b]	0.036[f]	8.7E-12 × exp(−615/T)[k]	1-butene[b]	0.039[e]	6.6E-12 × exp(465/T)[l]
n-butane[c]	0.077[f]	9.8E-12 × exp(−425/T)[l]	methylpropene[b]	0.012[e]	9.4E-12 × exp(505/T)[l]
n-pentane[c]	0.129[f]	1.81E-11 × exp(−452/T)[m]	trans-2-butene[b]	0.034[h]	1.0E-11 × exp(553/T)[l]
i-butane[c]	0.027[e]	7.0E-12 × exp(−350/T)[m]	cis-2-butene[b]	0.034[h]	1.1E-11 × exp(485/T)[l]
i-pentane[c]	0.075[e]	1.01E-11 × exp(−296/T)[m]	butandiene[b]	0.065[e]	1.58E-11 × exp(436/T)[n]
2,3-dimethylbutane[b]	0.061[e]	1.25E-11 × exp(−212/T)[m]			
2-methylpentane and 3-methylpentane[b]	0.11[e]	1.77E-11 × exp(−362/T)[m, q]	Aromatics		
hexane[b]	0.141[g]	1.98E-11 × exp(−394/T)[m]	benzene[d]	0.029[e]	2.3E-12 × exp(−190/T)[l]
heptane[b]	0.178[g]	2.76E-11 × exp(−430/T)[m]	propyl-benzene[b]	0.093[e]	5.8E-12[p]
			toluene[d]	0.08[e]	1.8E-12 × exp(340/T)[l]
Isoprene and derivatives			2-ethyltoluene[b]	0.106[e]	1.19E-11[p]
Isoprene[d]	0.117[i]	2.7E-11 × exp(390/T)[l]	3-ethyltoluene[b]	0.094[e]	1.86E-11[p]
methacrolein[c]	0.0705[i]	8.0E-12 × exp(380/T)[l]	4-ethyltoluene[b]	0.137[e]	1.18E-11[p]
methyl vinyl ketone[c]	0.11[i]	2.6E-12 × exp(610/T)[l]	o-xylene[c]	0.081[e]	1.36E-11[p]
			m-xylene and p-xylene[b]	0.085[e]	2.31E-11[p]
Monoterpenes			ethylbenzene[b]	0.072[e]	7.0E-12[p]
α-pinene[b]	0.18[j]	1.2E-11 × exp(440/T)[l]	1,3,5-trimethylbenzene[b]	0.127[e]	5.67E-11[p]
β-pinene[b]	0.18[j]	1.47E-11 × exp(467/T)[o]	1,2,4-trimethylbenzene[b]	0.105[e]	3.25E-11[p]
			1,2,3-trimethylbenzene[b]	0.119[e]	3.27E-11[p]
OVOC					
butanone[c]	0.015[e]	1.5E-12 × exp(−90/T)[l]			
butanal[c]	0.013[e]	6.0e-12 × exp(410/T)[l]			

[a] Tunable diode laser absorption spectroscopy; [b] Whole air sampling; [c] Gas chromatography – mass spectrometry; [d] Proton transfer reaction mass spectrometry; [e] MCM v3.2, may involve weighting by isomers; [f] Atkinson et al. (1982); [g] Arey et al. (2001); [h] O'Brien et al. (1998); [i] Paulot et al. (2009); [j] Nozière et al. (1999); [k] Sander et al. (2006); [l] Atkinson et al. (2006); [m] Calvert et al. (2008); [n] Li et al. (2006); [o] Gill and Hites (2002); [p] Calvert et al. (2002); [q] Rate for 2-methylpentane; [r] $k = k_\infty$ $k_o M/(k_o M + k_\infty) \times F_c^{1/j}$, $j = 1 + [\log(k_o M/k_\infty)/N]^2$, $\log = \log_{10}$

instantaneous production of ΣANs to HNO_3 for ten different possibilities (including our base case that was presented in the text). In the unique $RO_2 + RO_2$ rate case we take the rate of $RO_2 + RO_2$ reactions from MCM v3.2 $RO_2 + CH_3O_2$ rates for methyl vinyl ketone, methacrolein, isoprene, and monoterpenes. We weight the methyl vinyl ketone and isoprene rates by the initial branching of the different peroxy radicals. The monoterpene rate is calculated assuming an even split between α- and β-pinene and weighting the different peroxy radicals. No significant difference is observed using these rates. If we increase the isomerization rate of the isoprene peroxy radical by an order of magnitude (Isomerization × 10 case), we also observe no significant difference.

Recent measurements of the isoprene nitrate branching ratio range from 7 % to 12 % (Paulot et al., 2009; Lockwood et al., 2010). In our base calculation we use the branching ratio of 11.7 % reported by Paulot et al. (2009). In the 7 % IN case below, we use the yield of 7 % measured by Lockwood et al. (2010) and find that although the contribution from isoprene decreases, P(ΣANs) is still larger than P(HNO_3).

It is also likely that there are VOCs contributing to organic nitrate production that were not measured during ARCTAS, and thus the base calculation is biased low. For instance, only the monoterpenes α-pinene and β-pinene are measured. Measurements from the boreal forest in Finland indicate substantial contributions from other monoterpenes as well as contributions from sesquiterpenes (Spirig et al., 2004; Räisänen et al., 2009; Hakola et al., 2012). As expected, if we double the production from monoterpenes (2 × Monoterpenes) to account for unmeasured species, we see an increases in the ratio of P(ΣANs) to P(HNO_3).

Table A2. The median value of the P(ΣANs) to P(HNO_3) ratio and the speciation of P(ΣANs) for different assumptions regarding RO_2 reaction rates, OH and HO_2 concentrations, and VOC concentrations as described in Appendix A.

Case	P(ΣANs)/P(HNO_3)
Base	1.96
Unique $RO_2 + RO_2$ rate	1.84
Isomerization × 10	1.42
7 % IN	1.54
2 × Monoterpenes	2.57
HO_x CIMS OH	1.60
$[HO_2] \times 0.6$	2.83
HO_x CIMS HO_2	2.04
$[RO_2] \times 10$	1.82
Steady-state NO	3.00

In our base calculation we use the LIF OH measurement. It has recently been shown that this measurement may have an interference in environments with high biogenic emissions (Mao et al., 2012). This should have a minor effect on our calculation since any change in OH will affect both P(ΣANs) and P(HNO_3). Nevertheless, we test this possibility using the OH measurement from the chemical ionization mass spectrometry instrument (Cantrell et al., 2003) – the HO_x CIMS OH case. These two different measurements agreed well during the campaign (Ren et al., 2012). We see a slight decrease in the ratio of P(ΣANs) to P(HNO_3), however this can be attributed to the discrepancy in data coverage between the two instruments; if we restrict the LIF OH to the same points with CIMS OH coverage, we calculate the same median ratio.

Recently it has been reported that some LIF HO_2 measurements may suffer from a positive interference from the conversion of RO_2 to HO_2 in the instrument (Fuchs et al., 2011). This should increase our production of ΣANs relative to HNO_3 due to an increase in the fraction of RO_2 that reacts with NO. If we decrease the HO_2 by 40 % ($[HO_2] \times 0.6$) case, we find this to be true ($[HO_2] \times 0.6$ case). Using the HO_x CIMS HO_2 measurement also results in an insignificant change to the median P(ΣANs) to P(HNO_3).

In low NO_x environments it is possible that RO_2 is present in higher concentrations than HO_2 which would decrease our ΣANs production. However, we find that increasing the RO_2 concentration by an order of magnitude ($RO_2 \times 10$ case) has a negligible effect on our calculation. Even if this increase is coupled with a doubling of the $RO_2 + RO_2$ rate (not shown), there is no significant effect. Furthermore, the HO_x CIMS measurements of RO_2 do not show any evidence that the RO_2 to HO_2 ratio has any significant increase at low NO_x.

Lastly, we investigate the sensitivity of the calculation to the NO concentration. Using the NO concentration calculated assuming a steady-state between NO and NO_2 and the measured concentrations of NO_2, HO_2, O_3, NO_2 photolysis, and assuming that RO_2 is equal to HO_2 we find an increase in the median of the P(ΣANs) to P(HNO_3) ratio (Steady-state NO case). Overall, we conclude that although there is uncertainty in the absolute numbers, the production of ΣANs is, on average, faster than the production of HNO_3.

Appendix B

Uncertainty in the calculated ΣANs oxidation rate

The calculated oxidation rate of ΣANs is sensitive to uncertainties and assumptions including: the assumption that the instantaneous production represents the composition, possible interferences in HO_x measurements, reaction rate uncertainties, and assumptions regarding NO_x recycling.

Two of the most likely deviations from our assumption that the production in Fig. 4 represents the composition are nitrates produced from unmeasured BVOCS (likely monoterpenes and sesquiterpenes) and the presence of higher generation isoprene and monoterpene nitrates. In order for these nitrates to increase the ΣANs loss rate, their loss rate must, on a per molecule basis, be faster than the isoprene nitrate loss which implies that these nitrates are unsaturated. In Browne et al. (2013) we estimate the oxidation rates of unsaturated monoterpene nitrates 7.29×10^{-11} cm^3 molecules^{-1} s^{-1} for OH oxidation and 1.67×10^{-16} cm^3 molecules^{-1} s^{-1} for ozonolysis, similar to the isoprene nitrate oxidation rates. Thus, if the monoterpene nitrates had a larger NO_x recycling than the isoprene nitrates, then they would increase the ΣANs loss. NO_x recycling from monoterpene nitrates is difficult to estimate given the number of different monoterpene structures and the variability of emission factors between species. Furthermore, since the ozonolysis of the nitrates will dominate the loss process, NO_x recycling through this channel will be most important. To our knowledge, there are no measurement constraints on the NO_x recycling from the ozonolysis of any organic nitrate.

To estimate the effect of this complex problem we use results from the WRF-Chem model run over the boreal forest of Canada for the ARCTAS time period. This model uses a chemical mechanism with a comprehensive treatment of ΣANs including 11 isoprene-derived nitrates and two monoterpene-derived nitrates (one unsaturated and one saturated) as described in Browne et al. (2013) and Browne (2012). Sampled along the flight track, the WRF-Chem model predicts a ΣANs oxidative loss rate of 2.3×10^{-5} s^{-1} (median), a number similar to our estimate here, which suggests that these effects have only a small influence on our calculation.

Since the ozonolysis of isoprene nitrates accounts for the majority of the ΣANs loss rate, the possible interferences in the HO_x measurements (OH and HO_2) and uncertainties in the RO_2 reaction rates have a negligible effect on our calculated loss. Consequently, the uncertainties regarding isoprene nitrate ozonolysis, particularly the yields of the various

isoprene nitrate isomers, the ozonolysis rates, and the magnitude of the NO_x recycling are non-negligible. If we use the split between the δ-hydroxy and β-hydroxy nitrates from Lockwood et al. (2010) (with updates from Pratt et al., 2012) ($\sim 10\,\%$ and $\sim 90\,\%$, respectively) and the distribution of ΣANs production calculated using the isoprene nitrate formation yield from Lockwood et al. (2010) (51 % isoprene, 12 % MVK, 33 % α- and β-pinene), we calculate an overall ΣANs loss rate of $1.4 \times 10^{-5}\,s^{-1}$ assuming the slower β-hydroxy rate and $3.8 \times 10^{-5}\,s^{-1}$ if we assume the faster rate. These rates are similar to those in Table 2. We note that we have weighted the ozonolysis rates using the initial production yields of the β-hydroxy and δ-hydroxy nitrates. Given that these nitrates have (potentially) different atmospheric lifetimes (at 2×10^6 molecules cm^{-3} OH and 30 ppbv O_3 δ-hydroxy nitrates have a lifetime of ~ 1.2 h and the β-hydroxy nitrates of ~ 0.97–2.6 h using the OH rate constants from Paulot et al., 2009), it is likely that the reaction rate of the ΣANs we measure will favor the less reactive nitrates and our calculation may be high. Lastly, in our derivation of the NO_x recycling we follow the assumptions of MCM v3.2, which include the assumption of equal branching between the two possible carbonyl/Criegee biradical pairs. However, the exact branching depends on nature and number of the substituents on the alkene (Calvert et al., 2000).

There is also uncertainty introduced via our assumption that when the nitrooxy peroxy radical formed via OH oxidation reacts with HO_2 the nitrate functionality is preserved. Recent experimental work on the nitrooxy peroxy radicals derived from the reaction of isoprene with NO_3 indicates that the reaction of this peroxy radical with HO_2 likely has a large flux through the channel forming radical products (i.e. the alkoxy radical and OH) (Kwan et al., 2012). If we assume that this channel occurs half of the time, which is within the range estimated by Kwan et al. (2012), we calculate that the oxidation rate increases by 66 % when we assume the slower isoprene nitrate ozonolysis rate and 26 % when the faster rate is assumed.

It is also possible that reaction of the nitrooxy peroxy radical with other RO_2 (in particular, acyl peroxy radicals) may proceed at a faster rate. For instance, the reaction rate of $CH_3C(O)O_2$ with CH_3O_2 at 285 K is approximately two orders of magnitude faster than the self reaction rate of CH_3O_2 (Atkinson et al., 2006). If we increase the RO_2 rate constant by a factor of 50, an increase which is consistent with assuming that about half the peroxy radicals react with a rate of $2.3 \times 10^{-11}\,cm^3\,molecules^{-1}\,s^{-1}$ rather than $2.3 \times 10^{-13}\,cm^3\,molecules^{-1}\,s^{-1}$ (i.e. are more like acyl peroxy radicals), we calculate that the $RO_2 + RO_2$ reaction occurs $\sim 30\,\%$ of the time. This increases the oxidation rate to 2.2–$3.6 \times 10^{-5}\,s^{-1}$. We note that this likely overestimates the number of peroxy radicals. Furthermore, in our analysis we have assumed that the products of the nitrooxy peroxy radical reaction with other RO_2 are the same as those when it reacts with NO (i.e. we assume that the channel forming RO is dominant). While this channel is likely favored when the reaction is with an acyl peroxy radical, molecular channels which will retain the nitrate will likely be more important for non-acyl peroxy radicals. For instance, Kwan et al. (2012) estimate that only 19–38 % of the $RO_2 + RO_2$ reactions in their study result in the formation of alkoxy radicals. This decrease in alkoxy radical formation will also decrease the calculated oxidation rate.

Overall, these calculations suggest that ozonolysis of isoprene nitrates is the largest oxidation sink of organic nitrates. Further experimental constraints on the ozonolysis rates and products of the isoprene nitrates are needed to reduce the uncertainty concerning the fraction of NO_x that is recycled back to the atmosphere. Additional experiments constraining the products of isoprene-derived nitrooxy peroxy radicals with HO_2 and other peroxy radicals are also needed in order to understand the oxidation of these nitrates under low NO_x conditions.

Acknowledgements. The analysis described here was supported by NASA grant NNX08AR13G and a NASA Earth Systems Science Fellowship to ECB. MJC and JLJ were supported by NASA NNX08AD39G and NNX12AC03G. PTR-MS measurements were supported by the Austrian Research Promotion Agency (FFG-ALR) and the Tiroler Zukunftstiftung, and were carried out with the help/support of T. Mikoviny, M. Graus, A. Hansel and T. D. Maerk. We thank the NASA ground and flight crews for their hard work during ARCTAS.

Edited by: F. Keutsch

References

Apel, E. C., Hills, A. J., Lueb, R., Zindel, S., Eisele, S., and Riemer, D. D.: A fast-GC/MS system to measure C_2 to C_4 carbonyls and methanol aboard aircraft, J. Geophys. Res., 108, 8794, doi:10.1029/2002JD003199, 2003.

Arey, J., Aschmann, S. M., Kwok, E. S. C., and Atkinson, R.: Alkyl nitrate, hydroxyalkyl nitrate, and hydroxycarbonyl formation from the NO_x-air photooxidations of C5-C8 n-alkanes, J. Phys. Chem. A, 105, 1020–1027, doi:10.1021/jp003292z, 2001.

Atkinson, R., Aschmann, S. M., Carter, W. P. L., Winer, A. M., and Pitts, J. N.: Alkyl nitrate formation from the nitrogen oxide (NO_x)-air photooxidations of C2–C8 n-alkanes, J. Phys. Chem., 86, 4563–4569, doi:10.1021/j100220a022, 1982.

Atkinson, R., Baulch, D. L., Cox, R. A., Crowley, J. N., Hampson, R. F., Hynes, R. G., Jenkin, M. E., Rossi, M. J., Troe, J., and IUPAC Subcommittee: Evaluated kinetic and photochemical data for atmospheric chemistry: Volume II – gas phase reactions of organic species, Atmos. Chem. Phys., 6, 3625–4055, doi:10.5194/acp-6-3625-2006, 2006.

Barnes, I., Becker, K. H. and Zhu, T.: Near UV absorption spectra and photolysis products of difunctional organic nitrates: possible importance as NO_x reservoirs, J. Atmos. Chem., 17, 353–373, doi:10.1007/BF00696854, 1993.

Beaver, M. R., Clair, J. M. St., Paulot, F., Spencer, K. M., Crounse, J. D., LaFranchi, B. W., Min, K. E., Pusede, S. E., Wooldridge, P.

J., Schade, G. W., Park, C., Cohen, R. C., and Wennberg, P. O.: Importance of biogenic precursors to the budget of organic nitrates: observations of multifunctional organic nitrates by CIMS and TD-LIF during BEARPEX 2009, Atmos. Chem. Phys., 12, 5773–5785, doi:10.5194/acp-12-5773-2012, 2012.

Blake, N. J., Blake, D. R., Simpson, I. J., Meinardi, S., Swanson, A. L., Lopez, J. P., Katzenstein, A. S., Barletta, B., Shirai, T., Atlas, E., Sachse, G., Avery, M., Vay, S., Fuelberg, H. E., Kiley, C. M., Kita, K., and Rowland, F. S.: NMHCs and halocarbons in Asian continental outflow during the Transport and Chemical Evolution over the Pacific (TRACE-P) field campaign: comparison with PEM-West B, J. Geophys. Res., 108, 8806, doi:10.1029/2002JD003367, 2003.

Browne, E. C.: Observational constraints on the photochemistry of non-acyl peroxy nitrates and organic nitrates on regional and global scales, Ph. D. dissertation, University of California, Berkeley, USA, 2012.

Browne, E. C. and Cohen, R. C.: Effects of biogenic nitrate chemistry on the NO_x lifetime in remote continental regions, Atmos. Chem. Phys., 12, 11917–11932, doi:10.5194/acp-12-11917-2012, 2012.

Browne, E. C., Perring, A. E., Wooldridge, P. J., Apel, E., Hall, S. R., Huey, L. G., Mao, J., Spencer, K. M., Clair, J. M. St., Weinheimer, A. J., Wisthaler, A., and Cohen, R. C.: Global and regional effects of the photochemistry of $CH_3O_2NO_2$: evidence from ARCTAS, Atmos. Chem. Phys., 11, 4209–4219, doi:10.5194/acp-11-4209-2011, 2011.

Browne, E. C., Cohen, R. C. and et al.: Impacts of monoterpene nitrates on NO_x and NO_y in the Boreal forest, Atmos. Chem. Phys. Discuss., in preparation, 2013.

Calvert, J. G., Atkinson, R., Kerr, J. A., Madronich, S., and Moortgat, G. K.: The Mechanisms of Atmospheric Oxidation of the Alkenes, Oxford University Press, New York, 2000.

Calvert, J. G., Atkinson, R., Becker, K. H., Kamens, R. K., Seinfeld, J. H., Wallington, T. J., and Yarwood, G.: The Mechanisms of Atmospheric Oxidation of Aromatic Hydrocarbons, Oxford University Press, Oxford, New York, 2002.

Calvert, J. G., Derwent, R. G., Orlando, J. J., Tyndall, G. S., and Wallington, T. J.: Mechanisms of Atmospheric Oxidation of the Alkanes, Oxford University Press, Oxford, New York, 2008.

Cantrell, C. A., Edwards, G. D., Stephens, S., Mauldin, R. L., Zondlo, M. A., Kosciuch, E., Eisele, F. L., Shetter, R. E., Lefer, B. L., Hall, S., Flocke, F., Weinheimer, A., Fried, A., Apel, E., Kondo, Y., Blake, D. R., Blake, N. J., Simpson, I. J., Bandy, A. R., Thornton, D. C., Heikes, B. G., Singh, H. B., Brune, W. H., Harder, H., Martinez, M., Jacob, D. J., Avery, M. A., Barrick, J. D., Sachse, G. W., Olson, J. R., Crawford, J. H., and Clarke, A. D.: Peroxy radical behavior during the Transport and Chemical Evolution over the Pacific (TRACE-P) campaign as measured aboard the NASA P-3B aircraft, J. Geophys. Res., 108, 8797, doi:10.1029/2003JD003674, 2003.

Chen, X., Hulbert, D., and Shepson, P. B.: Measurement of the organic nitrate yield from OH reaction with isoprene, J. Geophys. Res., 103, 25563–25568, doi:10.1029/98JD01483, 1998.

Cleary, P. A., Wooldridge, P. J., and Cohen, R. C.: Laser-induced fluorescence detection of atmospheric NO_2 with a commercial diode laser and a supersonic expansion, Appl. Optics, 41, 6950–6956, 2002.

Cleary, P. A., Murphy, J. G., Wooldridge, P. J., Day, D. A., Millet, D. B., McKay, M., Goldstein, A. H., and Cohen, R. C.: Observations of total alkyl nitrates within the Sacramento Urban Plume, Atmos. Chem. Phys. Discuss., 5, 4801–4843, doi:10.5194/acpd-5-4801-2005, 2005.

Crounse, J. D., McKinney, K. A., Kwan, A. J., and Wennberg, P. O.: Measurement of gas-phase hydroperoxides by chemical ionization mass spectrometry, Anal. Chem., 78, 6726–6732, doi:10.1021/ac0604235, 2006.

Crounse, J. D., Paulot, F., Kjaergaard, H. G., and Wennberg, P. O.: Peroxy radical isomerization in the oxidation of isoprene, Phys. Chem. Chem. Phys., 13, 13607, doi:10.1039/c1cp21330j, 2011.

Crounse, J. D., Knap, H. C., Ørnsø, K. B., Jørgensen, S., Paulot, F., Kjaergaard, H. G., and Wennberg, P. O.: Atmospheric fate of methacrolein, 1: peroxy radical isomerization following addition of OH and O_2, J. Phys. Chem. A, 116, 5756–5762, doi:10.1021/jp211560u, 2012.

Cubison, M. J., Ortega, A. M., Hayes, P. L., Farmer, D. K., Day, D., Lechner, M. J., Brune, W. H., Apel, E., Diskin, G. S., Fisher, J. A., Fuelberg, H. E., Hecobian, A., Knapp, D. J., Mikoviny, T., Riemer, D., Sachse, G. W., Sessions, W., Weber, R. J., Weinheimer, A. J., Wisthaler, A., and Jimenez, J. L.: Effects of aging on organic aerosol from open biomass burning smoke in aircraft and laboratory studies, Atmos. Chem. Phys., 11, 12049–12064, doi:10.5194/acp-11-12049-2011, 2011.

Darer, A. I., Cole-Filipiak, N. C., O'Connor, A. E., and Elrod, M. J.: Formation and stability of atmospherically relevant isoprene-derived organosulfates and organonitrates, Environ. Sci. Technol., 45, 1895–1902, doi:10.1021/es103797z, 2011.

Day, D. A., Wooldridge, P. J., Dillon, M. B., Thornton, J. A., and Cohen, R. C.: A thermal dissociation laser-induced fluorescence instrument for in situ detection of NO_2, peroxy nitrates, alkyl nitrates, and HNO_3, J. Geophys. Res., 107, 4046, doi:10.1029/2001JD000779, 2002.

Day, D. A., Dillon, M. B., Wooldridge, P. J., Thornton, J. A., Rosen, R. S., Wood, E. C., and Cohen, R. C.: On alkyl nitrates, O_3, and the "missing NO_y", J. Geophys. Res., 108, 4501, doi:10.1029/2003JD003685, 2003.

Day, D. A., Wooldridge, P. J., and Cohen, R. C.: Observations of the effects of temperature on atmospheric HNO_3, ΣANs, ΣPNs, and NO_x: evidence for a temperature-dependent HO_x source, Atmos. Chem. Phys., 8, 1867–1879, doi:10.5194/acp-8-1867-2008, 2008.

Day, D. A., Liu, S., Russell, L. M., and Ziemann, P. J.: Organonitrate group concentrations in submicron particles with high nitrate and organic fractions in coastal southern California, Atmos. Environ., 44, 1970–1979, doi:10.1016/j.atmosenv.2010.02.045, 2010.

Donahue, N. M., Robinson, A. L., Stanier, C. O., and Pandis, S. N.: Coupled partitioning, dilution, and chemical aging of semivolatile organics, Environ. Sci. Technol., 40, 2635–2643, doi:10.1021/es052297c, 2006.

Faloona, I. C., Tan, D., Lesher, R. L., Hazen, N. L., Frame, C. L., Simpas, J. B., Harder, H., Martinez, M., Di Carlo, P., Ren, X., and Brune, W. H.: A laser-induced fluorescence instrument for detecting tropospheric OH and HO_2: characteristics and calibration, J. Atmos. Chem., 47, 139–167, doi:10.1023/B:JOCH.0000021036.53185.0e, 2004.

Farmer, D. K. and Cohen, R. C.: Observations of HNO_3, ΣAN, ΣPN and NO_2 fluxes: evidence for rapid HO_x chemistry within

a pine forest canopy, Atmos. Chem. Phys., 8, 3899–3917, doi:10.5194/acp-8-3899-2008, 2008.

Farmer, D. K., Matsunaga, A., Docherty, K. S., Surratt, J. D., Seinfeld, J. H., Ziemann, P. J., and Jimenez, J. L.: Response of an aerosol mass spectrometer to organonitrates and organosulfates and implications for atmospheric chemistry, P. Natl. Acad. Sci. USA, 109, 6670–6675, doi:10.1073/pnas.0912340107, 2010.

Farmer, D. K., Perring, A. E., Wooldridge, P. J., Blake, D. R., Baker, A., Meinardi, S., Huey, L. G., Tanner, D., Vargas, O., and Cohen, R. C.: Impact of organic nitrates on urban ozone production, Atmos. Chem. Phys., 11, 4085–4094, doi:10.5194/acp-11-4085-2011, 2011.

Fiore, A. M., Horowitz, L. W., Purves, D. W., II, H. L., Evans, M. J., Wang, Y., Li, Q., and Yantosca, R. M.: Evaluating the contribution of changes in isoprene emissions to surface ozone trends over the eastern United States, J. Geophys. Res., 110, D12303, doi:10.1029/2004JD005485, 2005.

Fiore, A. M., Levy II, H., and Jaffe, D. A.: North American isoprene influence on intercontinental ozone pollution, Atmos. Chem. Phys., 11, 1697–1710, doi:10.5194/acp-11-1697-2011, 2011.

Fry, J. L., Kiendler-Scharr, A., Rollins, A. W., Wooldridge, P. J., Brown, S. S., Fuchs, H., Dubé, W., Mensah, A., dal Maso, M., Tillmann, R., Dorn, H.-P., Brauers, T., and Cohen, R. C.: Organic nitrate and secondary organic aerosol yield from NO_3 oxidation of β-pinene evaluated using a gas-phase kinetics/aerosol partitioning model, Atmos. Chem. Phys., 9, 1431–1449, doi:10.5194/acp-9-1431-2009, 2009.

Fry, J. L., Kiendler-Scharr, A., Rollins, A. W., Brauers, T., Brown, S. S., Dorn, H.-P., Dubé, W. P., Fuchs, H., Mensah, A., Rohrer, F., Tillmann, R., Wahner, A., Wooldridge, P. J., and Cohen, R. C.: SOA from limonene: role of NO_3 in its generation and degradation, Atmos. Chem. Phys., 11, 3879–3894, doi:10.5194/acp-11-3879-2011, 2011.

Fuchs, H., Bohn, B., Hofzumahaus, A., Holland, F., Lu, K. D., Nehr, S., Rohrer, F., and Wahner, A.: Detection of HO_2 by laser-induced fluorescence: calibration and interferences from RO_2 radicals, Atmos. Meas. Tech., 4, 1209–1225, doi:10.5194/amt-4-1209-2011, 2011.

Fuentes, J. D., Gu, L., Lerdau, M., Atkinson, R., Baldocchi, D., Bottenheim, J. W., Ciccioli, P., Lamb, B., Geron, C., Guenther, A., Sharkey, T. D., and Stockwell, W.: Biogenic hydrocarbons in the atmospheric boundary layer: a review, Bull. Am. Meteorol. Soc., 81, 1537–1575, doi:10.1175/1520-0477(2000)081<1537:BHITAB>2.3.CO;2, 2000.

Fulton, D., Gillespie, T., Fuentes, J., and Wang, D.: Volatile organic compound emissions from young black spruce trees, Agr. Forest Meteorol., 90, 247–255, doi:10.1016/S0168-1923(97)00080-4, 1998.

Gill, K. J. and Hites, R. A.: Rate constants for the gas-phase reactions of the hydroxyl radical with isoprene, α- and β-pinene, and limonene as a function of temperature, J. Phys. Chem. A, 106, 2538–2544, doi:10.1021/jp013532q, 2002.

Hakola, H., Hellén, H., Hemmilä, M., Rinne, J., and Kulmala, M.: In situ measurements of volatile organic compounds in a boreal forest, Atmos. Chem. Phys., 12, 11665–11678, doi:10.5194/acp-12-11665-2012, 2012.

Henderson, B. H., Pinder, R. W., Crooks, J., Cohen, R. C., Carlton, A. G., Pye, H. O. T., and Vizuete, W.: Combining Bayesian methods and aircraft observations to constrain the $HO^{\cdot}$ + NO_2 reaction rate, Atmos. Chem. Phys., 12, 653–667, doi:10.5194/acp-12-653-2012, 2012.

Hofzumahaus, A., Rohrer, F., Lu, K., Bohn, B., Brauers, T., Chang, C.-C., Fuchs, H., Holland, F., Kita, K., Kondo, Y., Li, X., Lou, S., Shao, M., Zeng, L., Wahner, A., and Zhang, Y.: Amplified trace gas removal in the troposphere, Science, 324, 1702–1704, doi:10.1126/science.1164566, 2009.

Horii, C. V., William Munger, J., Wofsy, S. C., Zahniser, M., Nelson, D., and McManus, J. B.: Atmospheric reactive nitrogen concentration and flux budgets at a Northeastern US forest site, Agr. Forest Meteorol., 133, 210–225, doi:10.1016/j.agrformet.2004.08.009, 2005.

Horowitz, L. W., Liang, J., Gardner, G. M., and Jacob, D. J.: Export of reactive nitrogen from North America during summertime: sensitivity to hydrocarbon chemistry, J. Geophys. Res., 103, 13451–13476, doi:10.1029/97JD03142, 1998.

Horowitz, L. W., Fiore, A. M., Milly, G. P., Cohen, R. C., Perring, A., Wooldridge, P. J., Hess, P. G., Emmons, L. K., and Lamarque, J.-F.: Observational constraints on the chemistry of isoprene nitrates over the eastern United States, J. Geophys. Res., 112, D12S08, doi:10.1029/2006JD007747, 2007.

Hu, K. S., Darer, A. I., and Elrod, M. J.: Thermodynamics and kinetics of the hydrolysis of atmospherically relevant organonitrates and organosulfates, Atmos. Chem. Phys., 11, 8307–8320, doi:10.5194/acp-11-8307-2011, 2011.

Ito, A., Sillman, S., and Penner, J. E.: Global chemical transport model study of ozone response to changes in chemical kinetics and biogenic volatile organic compounds emissions due to increasing temperatures: Sensitivities to isoprene nitrate chemistry and grid resolution, J. Geophys. Res., 114, D09301, doi:10.1029/2008JD011254, 2009.

Jacob, D. J., Crawford, J. H., Maring, H., Clarke, A. D., Dibb, J. E., Emmons, L. K., Ferrare, R. A., Hostetler, C. A., Russell, P. B., Singh, H. B., Thompson, A. M., Shaw, G. E., McCauley, E., Pederson, J. R., and Fisher, J. A.: The Arctic Research of the Composition of the Troposphere from Aircraft and Satellites (ARCTAS) mission: design, execution, and first results, Atmos. Chem. Phys., 10, 5191–5212, doi:10.5194/acp-10-5191-2010, 2010.

Jenkin, M. E., Saunders, S. M., and Pilling, M. J.: The tropospheric degradation of volatile organic compounds: a protocol for mechanism development, Atmos. Environ., 31, 81–104, doi:10.1016/S1352-2310(96)00105-7, 1997.

Kwan, A. J., Chan, A. W. H., Ng, N. L., Kjaergaard, H. G., Seinfeld, J. H., and Wennberg, P. O.: Peroxy radical chemistry and OH radical production during the NO_3-initiated oxidation of isoprene, Atmos. Chem. Phys., 12, 7499–7515, doi:10.5194/acp-12-7499-2012, 2012.

Lelieveld, J., Butler, T. M., Crowley, J. N., Dillon, T. J., Fischer, H., Ganzeveld, L., Harder, H., Lawrence, M. G., Martinez, M., Taraborrelli, D., and Williams, J.: Atmospheric oxidation capacity sustained by a tropical forest, Nature, 452, 737–740, doi:10.1038/nature06870, 2008.

Li, Z., Nguyen, P., Fatima de Leon, M., Wang, J. H., Han, K., and He, G. Z.: Experimental and theoretical study of reaction of OH with 1,3-butadiene, J. Phys. Chem. A, 110, 2698–2708, doi:10.1021/jp0556557, 2006.

Liang, J., Horowitz, L. W., Jacob, D. J., Wang, Y., Fiore, A. M., Logan, J. A., Gardner, G. M., and Munger, J. W.: Seasonal budgets of reactive nitrogen species and ozone over the United States, and

export fluxes to the global atmosphere, J. Geophys. Res., 103, 13435–13450, doi:10.1029/97JD03126, 1998.

Liu, S., Shilling, J. E., Song, C., Hiranuma, N., Zaveri, R. A., and Russell, L. M.: Hydrolysis of organonitrate functional groups in aerosol particles, Aerosol Sci. Technol., 46, 1359–1369, 2012.

Lockwood, A. L., Filley, T. R., Rhodes, D., and Shepson, P. B.: Foliar uptake of atmospheric organic nitrates, Geophys. Res. Lett., 35, L15809, doi:10.1029/2008GL034714, 2008.

Lockwood, A. L., Shepson, P. B., Fiddler, M. N., and Alaghmand, M.: Isoprene nitrates: preparation, separation, identification, yields, and atmospheric chemistry, Atmos. Chem. Phys., 10, 6169–6178, doi:10.5194/acp-10-6169-2010, 2010.

Mao, J., Ren, X., Zhang, L., Van Duin, D. M., Cohen, R. C., Park, J.-H., Goldstein, A. H., Paulot, F., Beaver, M. R., Crounse, J. D., Wennberg, P. O., DiGangi, J. P., Henry, S. B., Keutsch, F. N., Park, C., Schade, G. W., Wolfe, G. M., Thornton, J. A., and Brune, W. H.: Insights into hydroxyl measurements and atmospheric oxidation in a California forest, Atmos. Chem. Phys., 12, 8009–8020, doi:10.5194/acp-12-8009-2012, 2012.

Mauldin III, R. L., Cantrell, C. A., Zondlo, M., Kosciuch, E., Eisele, F. L., Chen, G., Davis, D., Weber, R., Crawford, J., Blake, D., Bandy, A., and Thornton, D.: Highlights of OH, H_2SO_4, and methane sulfonic acid measurements made aboard the NASA P-3B during Transport and Chemical Evolution over the Pacific, J. Geophys. Res., 108, 8796, doi:10.1029/2003JD003410, 2003.

Mollner, A. K., Valluvadasan, S., Feng, L., Sprague, M. K., Okumura, M., Milligan, D. B., Bloss, W. J., Sander, S. P., Martien, P. T., Harley, R. A., McCoy, A. B., and Carter, W. P. L.: Rate of gas phase association of hydroxyl radical and nitrogen dioxide, Science, 330, 646–649, doi:10.1126/science.1193030, 2010.

Nozière, B., Barnes, I., and Becker, K.-H.: Product study and mechanisms of the reactions of α-pinene and of pinonaldehyde with OH radicals, J. Geophys. Res., 104, 23645–23,656, doi:10.1029/1999JD900778, 1999.

O'Brien, J. M., Czuba, E., Hastie, D. R., Francisco, J. S., and Shepson, P. B.: Determination of the hydroxy nitrate yields from the reaction of C2–C6 alkenes with OH in the presence of NO, J. Phys. Chem. A, 102, 8903–8908, doi:10.1021/jp982320z, 1998.

Pankow, J. F.: An absorption model of gas/particle partitioning of organic compounds in the atmosphere, Atmos. Environ., 28, 185–188, doi:10.1016/1352-2310(94)90093-0, 1994.

Paulot, F., Crounse, J. D., Kjaergaard, H. G., Kroll, J. H., Seinfeld, J. H., and Wennberg, P. O.: Isoprene photooxidation: new insights into the production of acids and organic nitrates, Atmos. Chem. Phys., 9, 1479–1501, doi:10.5194/acp-9-1479-2009, 2009.

Paulot, F., Henze, D. K., and Wennberg, P. O.: Impact of the isoprene photochemical cascade on tropical ozone, Atmos. Chem. Phys., 12, 1307–1325, doi:10.5194/acp-12-1307-2012, 2012.

Peeters, J. and Müller, J.-F.: HO_x radical regeneration in isoprene oxidation via peroxy radical isomerisations, II: experimental evidence and global impact, Phys. Chem. Chem. Phys., 12, 14227, doi:10.1039/c0cp00811g, 2010.

Peeters, J., Nguyen, T. L., and Vereecken, L.: HO_x radical regeneration in the oxidation of isoprene, Phys. Chem. Chem. Phys., 11, 5935, doi:10.1039/b908511d, 2009.

Perring, A. E., Bertram, T. H., Wooldridge, P. J., Fried, A., Heikes, B. G., Dibb, J., Crounse, J. D., Wennberg, P. O., Blake, N. J., Blake, D. R., Brune, W. H., Singh, H. B., and Cohen, R. C.: Airborne observations of total RONO2: new constraints on the yield and lifetime of isoprene nitrates, Atmos. Chem. Phys., 9, 1451–1463, doi:10.5194/acp-9-1451-2009, 2009.

Perring, A. E., Bertram, T. H., Farmer, D. K., Wooldridge, P. J., Dibb, J., Blake, N. J., Blake, D. R., Singh, H. B., Fuelberg, H., Diskin, G., Sachse, G., and Cohen, R. C.: The production and persistence of $\Sigma RONO_2$ in the Mexico City plume, Atmos. Chem. Phys., 10, 7215–7229, doi:10.5194/acp-10-7215-2010, 2010.

Pratt, K. A., Mielke, L. H., Shepson, P. B., Bryan, A. M., Steiner, A. L., Ortega, J., Daly, R., Helmig, D., Vogel, C. S., Griffith, S., Dusanter, S., Stevens, P. S., and Alaghmand, M.: Contributions of individual reactive biogenic volatile organic compounds to organic nitrates above a mixed forest, Atmos. Chem. Phys., 12, 10125–10143, doi:10.5194/acp-12-10125-2012, 2012.

Räisänen, T., Ryyppö, A., and Kellomäki, S.: Monoterpene emission of a boreal Scots pine (*Pinus sylvestris* L.) forest, Agr. Forest Meteorol., 149, 808–819, doi:10.1016/j.agrformet.2008.11.001, 2009.

Ren, X., Mao, J., Brune, W. H., Cantrell, C. A., Mauldin III, R. L., Hornbrook, R. S., Kosciuch, E., Olson, J. R., Crawford, J. H., Chen, G., and Singh, H. B.: Airborne intercomparison of HO_x measurements using laser-induced fluorescence and chemical ionization mass spectrometry during ARCTAS, Atmos. Meas. Tech., 5, 2025–2037, doi:10.5194/amt-5-2025-2012, 2012.

Roberts, J. M. and Fajer, R. W.: UV absorption cross sections of organic nitrates of potential atmospheric importance and estimation of atmospheric lifetimes, Environ. Sci. Technol., 23, 945–951, doi:10.1021/es00066a003, 1989.

Rollins, A. W., Kiendler-Scharr, A., Fry, J. L., Brauers, T., Brown, S. S., Dorn, H.-P., Dubé, W. P., Fuchs, H., Mensah, A., Mentel, T. F., Rohrer, F., Tillmann, R., Wegener, R., Wooldridge, P. J., and Cohen, R. C.: Isoprene oxidation by nitrate radical: alkyl nitrate and secondary organic aerosol yields, Atmos. Chem. Phys., 9, 6685–6703, doi:10.5194/acp-9-6685-2009, 2009.

Rollins, A. W., Fry, J. L., Hunter, J. F., Kroll, J. H., Worsnop, D. R., Singaram, S. W., and Cohen, R. C.: Elemental analysis of aerosol organic nitrates with electron ionization high-resolution mass spectrometry, Atmos. Meas. Tech., 3, 301–310, doi:10.5194/amt-3-301-2010, 2010a.

Rollins, A. W., Smith, J. D., Wilson, K. R., and Cohen, R. C.: Real time in situ detection of organic nitrates in atmospheric aerosols, Environ. Sci. Technol., 44, 5540–5545, doi:10.1021/es100926x, 2010b.

Rosen, R. S., Wood, E. C., Wooldridge, P. J., Thornton, J. A., Day, D. A., Kuster, W., Williams, E. J., Jobson, B. T., and Cohen, R. C.: Observations of total alkyl nitrates during Texas Air Quality Study 2000: implications for O_3 and alkyl nitrate photochemistry, J. Geophys. Res., 109, D07303, doi:10.1029/2003JD004227, 2004.

Sachse, G. W., Hill, G. F., Wade, L. O., and Perry, M. G.: Fast-response, high-precision carbon monoxide sensor using a tunable diode laser absorption technique, J. Geophys. Res., 92, 2071–2081, doi:10.1029/JD092iD02p02071, 1987.

Sander, S. P., Finlayson-Pitts,, J., Friedl, R. R., Golden, D. M., Huie, R. E., Keller-Rudek, H., Kolb, C. E., Kurylo, M. J., Molina, M. J., Moortgat, G. K., Orkin, V. L., Ravishankara, A. R., and Wine, P. H.: Chemical kinetics and photochemical data for use in atmospheric studies, Evaluation No.

15, JPL Publication 06-2, Jet Propulsion Laboratory, Pasadena, 2006, available at: http://jpldataeval.jpl.nasa.gov, 2006.

Sato, K.: Detection of nitrooxypolyols in secondary organic aerosol formed from the photooxidation of conjugated dienes under high-NO_x conditions, Atmos. Environ., 42, 6851–6861, doi:10.1016/j.atmosenv.2008.05.010, 2008.

Saunders, S. M., Jenkin, M. E., Derwent, R. G., and Pilling, M. J.: Protocol for the development of the Master Chemical Mechanism, MCM v3 (Part A): tropospheric degradation of non-aromatic volatile organic compounds, Atmos. Chem. Phys., 3, 161–180, doi:10.5194/acp-3-161-2003, 2003.

Seinfeld, J. H. and Pandis, S. N.: Atmospheric Chemistry and Physics: from Air Pollution to Climate Change, 2nd edn., Wiley, Hoboken, NJ, 2006.

Shashkov, A., Higuchi, K., and Chan, D.: Aircraft vertical profiling of variation of CO_2 over a Canadian Boreal Forest site: a role of advection in the changes in the atmospheric boundary layer CO_2 content, Tellus B, 59, 234–243, doi:10.1111/j.1600-0889.2006.00237.x, 2007.

Shepson, P. B., Mackay, E., and Muthuramu, K.: Henry's law constants and removal processes for several atmospheric β-hydroxy alkyl nitrates, Environ. Sci. Technol., 30, 3618–3623, doi:10.1021/es960538y, 1996.

Simpson, I. J., Akagi, S. K., Barletta, B., Blake, N. J., Choi, Y., Diskin, G. S., Fried, A., Fuelberg, H. E., Meinardi, S., Rowland, F. S., Vay, S. A., Weinheimer, A. J., Wennberg, P. O., Wiebring, P., Wisthaler, A., Yang, M., Yokelson, R. J., and Blake, D. R.: Boreal forest fire emissions in fresh Canadian smoke plumes: $C-1–C_{10}$ volatile organic compounds (VOCs), CO_2, CO, NO_2, NO, HCN and CH_3CN, Atmos. Chem. Phys., 11, 6445–6463, doi:10.5194/acp-11-6445-2011, 2011.

Slowik, J. G., Stroud, C., Bottenheim, J. W., Brickell, P. C., Chang, R. Y.-W., Liggio, J., Makar, P. A., Martin, R. V., Moran, M. D., Shantz, N. C., Sjostedt, S. J., van Donkelaar, A., Vlasenko, A., Wiebe, H. A., Xia, A. G., Zhang, J., Leaitch, W. R., and Abbatt, J. P. D.: Characterization of a large biogenic secondary organic aerosol event from eastern Canadian forests, Atmos. Chem. Phys., 10, 2825–2845, doi:10.5194/acp-10-2825-2010, 2010.

Spirig, C., Guenther, A., Greenberg, J. P., Calanca, P., and Tarvainen, V.: Tethered balloon measurements of biogenic volatile organic compounds at a Boreal forest site, Atmos. Chem. Phys., 4, 215–229, doi:10.5194/acp-4-215-2004, 2004.

Stavrakou, T., Peeters, J., and Müller, J.-F.: Improved global modelling of HO_x recycling in isoprene oxidation: evaluation against the GABRIEL and INTEX-A aircraft campaign measurements, Atmos. Chem. Phys., 10, 9863–9878, doi:10.5194/acp-10-9863-2010, 2010.

Stone, D., Evans, M. J., Edwards, P. M., Commane, R., Ingham, T., Rickard, A. R., Brookes, D. M., Hopkins, J., Leigh, R. J., Lewis, A. C., Monks, P. S., Oram, D., Reeves, C. E., Stewart, D., and Heard, D. E.: Isoprene oxidation mechanisms: measurements and modelling of OH and HO_2 over a South-East Asian tropical rainforest during the OP3 field campaign, Atmos. Chem. Phys., 11, 6749–6771, doi:10.5194/acp-11-6749-2011, 2011.

Suarez-Bertoa, R., Picquet-Varrault, B., Tamas, W., Pangui, E., and Doussin, J.-F.: Atmospheric fate of a series of carbonyl nitrates: photolysis frequencies and OH-oxidation rate constants, Environ. Sci. Technol., 46, 12502–12509, doi:10.1021/es302613x, 2012.

Talukdar, R. K., Burkholder, J. B., Hunter, M., Gilles, M. K., Roberts, J. M., and Ravishankara, A. R.: Atmospheric fate of several alkyl nitrates, part 2: UV absorption cross-sections and photodissociation quantum yields, J. Chem. Soc.-Faraday Trans., 93, 2797–2805, doi:10.1039/a701781b, 1997.

Taraborrelli, D., Lawrence, M. G., Crowley, J. N., Dillon, T. J., Gromov, S., Groß, C. B. M., Vereecken, L., and Lelieveld, J.: Hydroxyl radical buffered by isoprene oxidation over tropical forests, Nat. Geosci., 5, 190–193, doi:10.1038/ngeo1405, 2012.

Thaler, R. D., Mielke, L. H., and Osthoff, H. D.: Quantification of nitryl chloride at part per trillion mixing ratios by thermal dissociation cavity ring-down spectroscopy, Anal. Chem., 83, 2761–2766, doi:10.1021/ac200055z, 2011.

Thornton, J. A., Wooldridge, P. J., and Cohen, R. C.: Atmospheric NO_2: in situ laser-induced fluorescence detection at parts per trillion mixing ratios, Anal. Chem., 72, 528–539, doi:10.1021/ac9908905, 2000.

Thornton, J. A., Wooldridge, P. J., Cohen, R. C., Martinez, M., Harder, H., Brune, W. H., Williams, E. J., Roberts, J. M., Fehsenfeld, F. C., Hall, S. R., Shetter, R. E., Wert, B. P., and Fried, A.: Ozone production rates as a function of NO_x abundances and HO_x production rates in the Nashville urban plume, J. Geophys. Res.-Atmos., 107, 4146, doi:10.1029/2001JD000932, 2002.

Trainer, M., Buhr, M. P., Curran, C. M., Fehsenfeld, F. C., Hsie, E. Y., Liu, S. C., Norton, R. B., Parrish, D. D., Williams, E. J., Gandrud, B. W., Ridley, B. A., Shetter, J. D., Allwine, E. J., and Westberg, H. H.: Observations and modeling of the reactive nitrogen photochemistry at a rural site, J. Geophys. Res., 96, 3045–3063, doi:10.1029/90JD02395, 1991.

Treves, K., Shragina, L., and Rudich, Y.: Henry's law constants of some β-, γ-, and δ-hydroxy alkyl nitrates of atmospheric interest, Environ. Sci. Technol., 34, 1197–1203, doi:10.1021/es990558a, 2000.

Vereecken, L. and Peeters, J.: Nontraditional (per)oxy ring-closure paths in the atmospheric oxidation of isoprene and monoterpenes, J. Phys. Chem. A, 108, 5197–5204, doi:10.1021/jp049219g, 2004.

von Kuhlmann, R., Lawrence, M. G., Pöschl, U., and Crutzen, P. J.: Sensitivities in global scale modeling of isoprene, Atmos. Chem. Phys., 4, 1–17, doi:10.5194/acp-4-1-2004, 2004.

Weaver, C. P., Cooter, E., Gilliam, R., Gilliland, A., Grambsch, A., Grano, D., Hemming, B., Hunt, S. W., Nolte, C., Winner, D. A., Liang, X.-Z., Zhu, J., Caughey, M., Kunkel, K., Lin, J.-T., Tao, Z., Williams, A., Wuebbles, D. J., Adams, P. J., Dawson, J. P., Amar, P., He, S., Avise, J., Chen, J., Cohen, R. C., Goldstein, A. H., Harley, R. A., Steiner, A. L., Tonse, S., Guenther, A., Lamarque, J.-F., Wiedinmyer, C., Gustafson, W. I., Leung, L. R., Hogrefe, C., Huang, H.-C., Jacob, D. J., Mickley, L. J., Wu, S., Kinney, P. L., Lamb, B., Larkin, N. K., McKenzie, D., Liao, K.-J., Manomaiphiboon, K., Russell, A. G., Tagaris, E., Lynn, B. H., Mass, C., Salathé, E., O'Neill, S. M., Pandis, S. N., Racherla, P. N., Rosenzweig, C., and Woo, J.-H.: A preliminary synthesis of modeled climate change impacts on US regional ozone concentrations, Bull. Am. Meteorol. Soc., 90, 1843–1863, doi:10.1175/2009BAMS2568.1, 2009.

Weinheimer, A. J., Walega, J. G., Ridley, B. A., Gary, B. L., Blake, D. R., Blake, N. J., Rowland, F. S., Sachse, G. W., Anderson, B. E., and Collins, J. E.: Meridional distributions of NO_x, NO_y, and other species in the lower stratosphere and upper tro-

posphere during AASE II, Geophys. Res. Lett., 21, 2583–2586, doi:10.1029/94GL01897, 1994.

Whalley, L. K., Edwards, P. M., Furneaux, K. L., Goddard, A., Ingham, T., Evans, M. J., Stone, D., Hopkins, J. R., Jones, C. E., Karunaharan, A., Lee, J. D., Lewis, A. C., Monks, P. S., Moller, S. J., and Heard, D. E.: Quantifying the magnitude of a missing hydroxyl radical source in a tropical rainforest, Atmos. Chem. Phys., 11, 7223–7233, doi:10.5194/acp-11-7223-2011, 2011.

Wisthaler, A., Hansel, A., Dickerson, R. R., and Crutzen, P. J.: Organic trace gas measurements by PTR-MS during INDOEX 1999, J. Geophys. Res., 107, 8024, doi:10.1029/2001JD000576, 2002.

Wooldridge, P. J., Perring, A. E., Bertram, T. H., Flocke, F. M., Roberts, J. M., Singh, H. B., Huey, L. G., Thornton, J. A., Wolfe, G. M., Murphy, J. G., Fry, J. L., Rollins, A. W., LaFranchi, B. W., and Cohen, R. C.: Total Peroxy Nitrates (ΣPNs) in the atmosphere: the Thermal Dissociation-Laser Induced Fluorescence (TD-LIF) technique and comparisons to speciated PAN measurements, Atmos. Meas. Tech., 3, 593–607, doi:10.5194/amt-3-593-2010, 2010.

Wu, S., Mickley, L. J., Jacob, D. J., Logan, J. A., Yantosca, R. M., and Rind, D.: Why are there large differences between models in global budgets of tropospheric ozone?, J. Geophys. Res., 112, D05302, doi:10.1029/2006JD007801, 2007.

Zuend, A., Marcolli, C., Booth, A. M., Lienhard, D. M., Soonsin, V., Krieger, U. K., Topping, D. O., McFiggans, G., Peter, T., and Seinfeld, J. H.: New and extended parameterization of the thermodynamic model AIOMFAC: calculation of activity coefficients for organic-inorganic mixtures containing carboxyl, hydroxyl, carbonyl, ether, ester, alkenyl, alkyl, and aromatic functional groups, Atmos. Chem. Phys., 11, 9155–9206, doi:10.5194/acp-11-9155-2011, 2011.